Use-dependent block of the voltage-gated Na^+ channel by tetrodotoxin and saxitoxin: Effect of pore mutations that change ionic selectivity

Chien-Jung Huang,[1] Laurent Schild,[2] and Edward G. Moczydlowski[3,4]

[1]Vertex Pharmaceuticals Inc., San Diego, CA 92121
[2]Institut de Pharmacologie et Toxicologie de l'Université, CH-1005 Lausanne, Switzerland
[3]Nanobiology Department, Sandia National Laboratories, Albuquerque, NM 87185
[4]Department of Biochemistry and Molecular Biology, The University of New Mexico School of Medicine, Albuquerque, NM 87131

Voltage-gated Na^+ channels (NaV channels) are specifically blocked by guanidinium toxins such as tetrodotoxin (TTX) and saxitoxin (STX) with nanomolar to micromolar affinity depending on key amino acid substitutions in the outer vestibule of the channel that vary with NaV gene isoforms. All NaV channels that have been studied exhibit a use-dependent enhancement of TTX/STX affinity when the channel is stimulated with brief repetitive voltage depolarizations from a hyperpolarized starting voltage. Two models have been proposed to explain the mechanism of TTX/STX use dependence: a conformational mechanism and a trapped ion mechanism. In this study, we used selectivity filter mutations (K1237R, K1237A, and K1237H) of the rat muscle NaV1.4 channel that are known to alter ionic selectivity and Ca^{2+} permeability to test the trapped ion mechanism, which attributes use-dependent enhancement of toxin affinity to electrostatic repulsion between the bound toxin and Ca^{2+} or Na^+ ions trapped inside the channel vestibule in the closed state. Our results indicate that TTX/STX use dependence is not relieved by mutations that enhance Ca^{2+} permeability, suggesting that ion–toxin repulsion is not the primary factor that determines use dependence. Evidence now favors the idea that TTX/STX use dependence arises from conformational coupling of the voltage sensor domain or domains with residues in the toxin-binding site that are also involved in slow inactivation.

The Journal of General Physiology

INTRODUCTION

Ion channel proteins confer complex electrical behavior to cell membranes that underlies animate behaviors such as sensation and memory. One of the simplest forms of memory is a channel protein molecule that appears to remember a previous chemical or electrical event as observed by a transient change in its functional activity. The voltage-gated Na^+ channel (NaV channel) offers a striking example of molecular memory in its conversion to inexcitable fast and slow inactivated forms of itself after being stimulated by depolarizing voltage pulses of various duration (Goldin 2003; Ulbricht 2005). Besides gating behavior that depends on past history of molecular experiences (e.g., voltage and phosphorylation) NaV channels are also well known for memory-like use-dependent behavior of drugs (e.g., local anesthetics and antiarrhythmics; Hille 1977; Fozzard et al., 2011) and toxins such as tetrodotoxin (TTX) and saxitoxin (STX; Cervenka et al., 2010).

Use dependence of local anesthetics such as lidocaine has been extensively studied given its clinical significance for suppression of hyperexcitability associated with pain, arrhythmia, and epilepsy. Biophysical experiments have shown that electrostatic neutralization by trifluorination of a single Phe residue in the DIV-S6 transmembrane segment (Phe1579 in NaV1.4) largely eliminates use dependence of lidocaine block (Ahern et al., 2008a). This work has led to a conformational hypothesis to explain use dependence of local anesthetic block that involves a cation–π interaction between the cationic drug and the aromatic ring of Phe1579 exposed to the internal ion conduction pathway formed by four S6 transmembrane segments (Ahern et al., 2008b). Gating current measurements have further shown that local anesthetic block mediated by interaction with Phe1759 of heart NaV1.5 (equivalent to Phe1579 of muscle NaV1.4) is coupled to charge immobilization or stabilization of the S4 voltage sensor elements of homologous domains DIII and DIV in an outward depolarized position (Hanck et al., 2009; Fozzard et al., 2011).

TTX and STX are small natural cyclic guanidinium molecules prized for their specificity in blocking NaV channels (Llewellyn, 2006; Lee and Ruben, 2008, Fozzard and Lipkind, 2010). TTX blocks all nine gene isoforms

Correspondence to Edward G. Moczydlowski: egmoczy@sandia.gov

Abbreviations used in this paper: BTX, batrachotoxin; NaV channel, voltage-gated Na^+ channel; STX, saxitoxin; TTX, tetrodotoxin.

The Rockefeller University Press $30.00
J. Gen. Physiol. Vol. 140 No. 4 435–454
www.jgp.org/cgi/doi/10.1085/jgp.201210853

of mammalian NaV channels with an affinity ranging from nanomolar to micromolar depending on substitutions of key residues located in the external vestibule leading to the narrow pore entrance (Lee and Ruben, 2008). Similarly, natural derivatives of STX that differ by small polar chemical substituents block NaV channels with nanomolar to micromolar affinity depending on chemical interactions with many of the same channel residues that determine TTX affinity (Guo et al., 1987; Favre et al., 1995; Penzotti et al., 1998, 2001; Choudhary et al., 2002).

This paper concerns a memory-like feature of TTX/STX block first observed for heart and squid NaV channels (Baer et al., 1976; Gage et al., 1976; Cohen et al., 1981). This toxin block phenomenon has been variously described as use-dependent, phasic, or postrepolarization block (Cohen et al., 1981; Makielski et al., 1993) and is somewhat analogous to use-dependent behavior of local anesthetics. Use-dependent block by TTX/STX is characterized by an approximately three- to fivefold increase in toxin affinity (or decrease in IC_{50}) as compared with first-pulse tonic or resting block from a hyperpolarized holding voltage (e.g., −100 mV) that develops in response to brief repetitive depolarization (e.g., voltage pulses to −10 mV; Conti et al., 1996; Boccaccio et al., 1999; Moran et al., 2003). Such an increase in TTX/STX affinity can be evoked by a single depolarizing voltage pulse as brief as 1 ms (Salgado et al., 1986; Eickhorn et al., 1990). The biphasic kinetics of development and recovery of the increase in TTX/STX affinity after the channel experiences a positive voltage pulse have been tracked by following the current response to test pulses delivered after return from subsequent intervals of hyperpolarized voltage (Salgado et al., 1986; Patton and Goldin, 1991; Makielski et al., 1993; Conti et al., 1996; Boccaccio et al., 1999). Use dependence appears to be a universal feature of TTX/STX block as documented for NaV channels from squid axon (Gage et al., 1976), crayfish nerve (Salgado et al., 1986), frog nerve (Lönnendonker, 1989), mammalian heart (Cohen et al., 1981; Eickhorn et al., 1990; Makielski et al., 1993; Satin et al., 1994a; Dumaine and Hartmann, 1996), rat brain (Patton and Goldin, 1991; Satin et al., 1994a; Conti et al., 1996), and rat skeletal muscle (Moran et al., 2003).

Mechanistic work has led to two plausible hypotheses to explain the use-dependent increase in TTX/STX affinity. The first hypothesis (conformational hypothesis) proposes that use-dependent toxin block arises from a change in the TTX/STX-binding site from a low-affinity conformation at hyperpolarized membrane potential with channels in the closed resting state to a high-affinity conformation that develops in certain closed states on the voltage activation pathway to channel opening (Patton and Goldin, 1991; Makielski et al., 1993; Satin et al., 1994a; Dumaine and Hartmann, 1996). The second hypothesis (ion interaction or trapped ion hypothesis) proposes that low affinity for TTX/STX at hyperpolarized holding voltage is caused by a repulsive electrostatic interaction between TTX^{1+}/STX^{2+} and Ca^{2+} or Na^{+} ions trapped between the bound pore-blocking toxin and the inner activation gate of the closed channel (Salgado et al., 1986; Conti et al., 1996; Boccaccio et al., 1999; Moran et al., 2003). In the latter hypothesis, the higher affinity for TTX/STX that develops with brief depolarization is thought to result from the escape of trapped Ca^{2+} or Na^{+} to the inside of the cell membrane upon opening of the activation gate during the voltage pulse.

Although previous attempts to discriminate these hypotheses have explored the effects of a variety of NaV channel mutations (Patton and Goldin, 1991; Satin et al., 1994a; Dumaine and Hartmann, 1996; Boccaccio et al., 1999; Santarelli et al., 2007a), the effect of mutations of the selectivity filter (or DEKA locus) known to change the ionic selectivity of NaV channels for Na^{+}, K^{+}, and Ca^{2+} (Heinemann et al., 1992b; Favre et al., 1996; Schlief et al., 1996) has not been previously described. In particular, mutations of K1237 (rat NaV1.4 residue numbering) in DIII of the DEKA locus are known to lower the energy barrier to Ca^{2+} permeation. Such mutants (e.g., K1237A) exhibit large inward current for Ca^{2+}, a divalent cation which does not conduct measurable current in native NaV channels (Heinemann et al., 1992b; Favre et al., 1996; Schlief et al., 1996; Sun et al., 1997). Because mutations that facilitate inward movement of cations and change ionic selectivity in the vicinity of the toxin-binding site would be most likely to change the affinity and/or number of Ca^{2+} and Na^{+} ions involved in the trapped ion mechanism, we decided to examine the effect of three mutations (K1237R, K1237A, and K1237H) of the critical DIII-K1237 residue known to dramatically alter ionic selectivity. Our results and other recent findings suggest that interactions between inorganic ions and bound TTX/STX may be less important for the underlying mechanism of use dependence than conformational changes of the toxin-binding site coupled to the voltage dependence of channel activation.

MATERIALS AND METHODS

Channel expression and cell culture

Wild-type and mutant (K1237R, K1237H, and K1237A) clones of the rat skeletal muscle NaV1.4 (μ1) channel were constructed, subcloned, and stably expressed in HEK293 cells as previously described (Favre et al., 1996; Sun et al., 1997; Huang et al., 2000). Based on the single letter code for conserved selectivity filter residues in each of four homologous repeat domains DI–DIV, these mutants are also denoted, respectively, as DEKA (wild type), DERA, DEHA, and DEAA. Stably transfected cell lines were maintained in Dulbecco's modified essential medium (Life Technologies) supplemented with 10% fetal bovine serum and 500 μg/l Geneticin (Life Technologies), incubated in a humidified 5% CO_2/95% O_2 atmosphere at 37°C, and subcultured every 3–4 d. Cells were plated onto small chips of regular glass coverslips for whole-cell recordings or poly-lysine–coated glass coverslips for inside-out recordings.

Solutions and electrophysiology

The standard extracellular Na^+ bath solution for whole-cell recording was 140 mM NaCl, 3 mM KCl, 2 mM $MgCl_2$, 2 mM $CaCl_2$, 10 mM glucose, and 10 mM Hepes-NaOH, pH 7.3. The intracellular Cs^+/Na^+ pipette solution was 125 mM CsF, 2 mM $MgCl_2$, 1.1 mM EGTA, 10 mM glucose, and 20 Na^+-Hepes, pH 7.3. For experiments on Ca^{2+} dependence of toxin block, the bath solutions contained 0.2, 0.5, 1, 2, or 5 mM $CaCl_2$, 140 mM NaCl, 3 mM KCl, 10 mM glucose, and 10 mM Hepes-NaOH, pH 7.3. Inside-out macropatch recordings were made under conditions of nearly symmetrical $[Na^+]$: extracellular pipette solution of 140 mM NaCl, 3 mM KCl, 2 mM $MgCl_2$, 2 mM $CaCl_2$, 10 mM glucose, and 10 mM Hepes-NaOH, pH 7.3; and intracellular bath solution of 120 mM NaF, 20 mM NaH_2PO_4, 1.1 mM EGTA, and 10 mM glucose, pH 7.3, with NaOH. TTX was purchased from EMD Millipore, μ-conotoxin GIIIA (μ-CTX) was purchased from Bachem, and STX was supplied by S. Hall of the U.S. Food and Drug Administration.

Patch electrodes were fabricated from Kimax-51 borosilicate capillaries (Thermo Fisher Scientific) and pulled with a two-stage puller (PP-83; Narishige Scientific Instrument Laboratory). The resistance of whole-cell patch pipettes was 1–2 MΩ when filled with Cs^+/Na^+ solution, and that of inside-out patch pipettes was 0.5–0.7 MΩ when filled with extracellular Na^+ pipette solution. Recordings of macroscopic Na^+ currents were performed at room temperature (23°C), using an EPC-9 amplifier (HEKA) and Pulse and Pulse-fit software (Instrutech). The recorded data were sampled at a rate of 50 kHz, filtered at 10 kHz, and subsequently low-pass filtered at 3 kHz for analysis and presentation. An online P/4 protocol delivered at −140 mV was used to subtract capacitance transients and leak currents, except for experiments using high-frequency (167 Hz) test protocols. Series resistance in whole-cell experiments was electronically compensated to at least 70%. A KCl-agar bridge was used to connect the bath to the Ag/AgCl ground electrode.

Data collection commenced after voltage-activated Na^+ current exhibited a stable response during continuous perfusion of control bath solution driven by gravity. The waiting period for whole-cell recording was usually 15–20 min from the time of membrane break-in or ∼5–8 min after membrane patch excision for inside-out recordings. Typical wash-in/wash-out experiments for measuring tonic (resting) block were monitored with a consecutive train of 10-ms test pulses to −10 mV, delivered at a low frequency of 1/30 s from a holding potential of −120 mV. Use dependence of toxin block was assessed with 50-s trains of 10-ms pulses to −10 mV, delivered at intervals of 10, 5, 2, 1, 0.5, and 0.25 s from a holding potential of −120 mV. Pulse protocols with varied pulse intervals are, respectively, denoted as $f_{1/30}$, $f_{0.1}$, $f_{0.2}$, $f_{0.5}$, f_1, f_2, and f_4, with subscripts indicating frequency (hertz) of stimulation. Successive trials were separated by a 3-min recovery period at −120 mV, monitored at $f_{1/30}$. In some experiments with DEHA and DEAA mutant channels (see Figs. 3, 4, and 9), a high-frequency train (denoted as f_{167}) of 1-ms pulses to −10 mV, delivered at 5-ms intervals (i.e., one voltage pulse every 6 ms) from −120 mV, was necessary to resolve the rapid time course of use-dependent block. Use-dependent block for inside-out patch recordings was monitored with 50-s trains of 3.25-ms test pulses to −30, 50, or 100 mV, delivered at f_4 from −120 mV.

Data analysis

The time course of use-dependent block was fit to a single exponential function, and steady-state toxin inhibition titrations were fit to a one-site binding isotherm using SigmaPlot software (Systat Software Inc.). For the purpose of presentation, current data for DEKA and DERA channels illustrating the time dependence of toxin block were either normalized to the mean value of inward peak currents before perfusion of toxin (I/I_0; see Figs. 1, 5, 8 A, and 11) or to the value of peak current elicited by the first pulse of each stimulation from the same cell/patch (I/I_1; see Figs. 2; 3; 4; 9, A and B; and 10). However, DEHA and DEAA mutant channels exhibited pronounced cumulative inactivation marked by significant decline of inward peak current at a stimulation frequency of 167 Hz (see Figs. 3 and 4) in the absence of toxin.

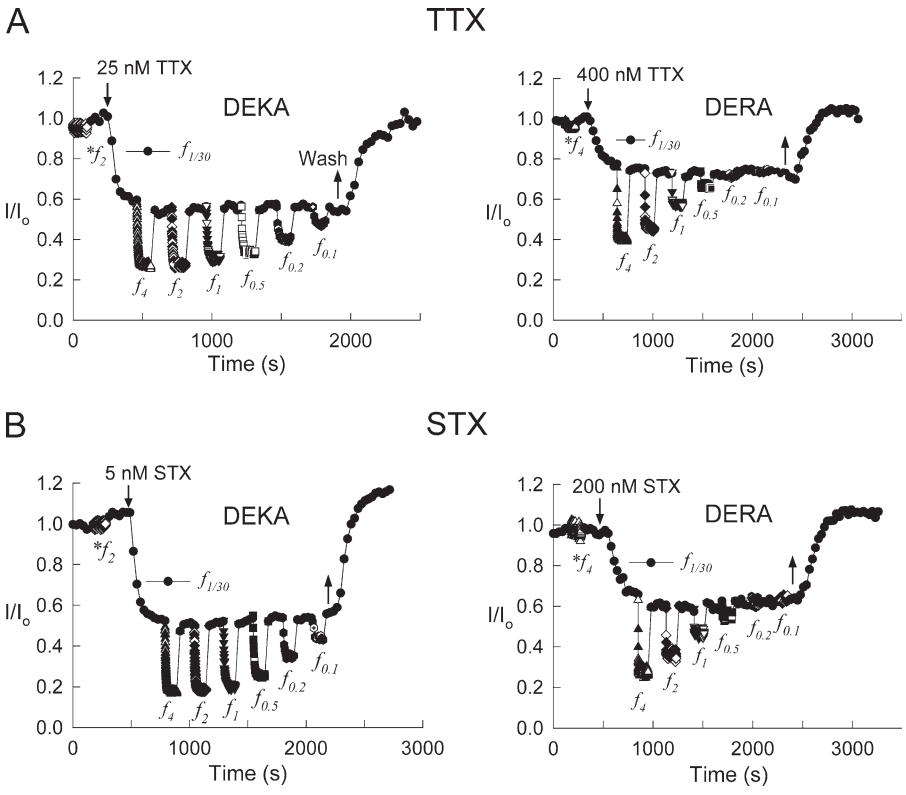

Figure 1. Typical wash-in and wash-out experiments of DEKA wild-type and DERA mutant channels for TTX and STX. (A and B) Data points are normalized peak whole-cell currents elicited by consecutive 10-ms pulses to −10 mV from a holding potential of −120 mV, delivered at rate of 1/30 ($f_{1/30}$) Hz interspersed with 50-s trains of pulses at 0.1 ($f_{0.1}$), 0.2 ($f_{0.2}$), 0.5 ($f_{0.5}$), 1 (f_1), 2 (f_2), or 4 (f_4) Hz, in the presence of the indicated concentrations of TTX or STX. Use-dependent behavior is similar for TTX and STX; however, the toxin-binding affinity and use-dependent kinetics of the two channel types are markedly different. Data periods labeled as $*f_2$ and $*f_4$ denote onset of 50-s control pulse trains for toxin-free bath solution.

For these mutants, the following method described by Boccaccio et al. (1999) was used for normalization. Assuming the kinetics of frequency-dependent current decline in the absence of toxin is independent of toxin binding, the time dependence of toxin block can be expressed as the ratio of peak currents collected in the presence of TTX to those collected with the same pulse protocol in the absence of toxin. This ratio is subsequently normalized to 1.0 by dividing by the +TTX/−TTX current ratio for the first pulse. Except for the results illustrating the response of a typical cell (see Figs. 1; 2; 9, A and B; and 11), all data points are presented as the mean ± SE for 3–10 cells/patches.

RESULTS

Effect of mutations that alter ionic selectivity on the kinetics of TTX/STX use dependence

To investigate the possible relationship of use-dependent block by TTX/STX to binding and discrimination of inorganic cations by the NaV channel selectivity filter, we studied voltage-activated Na^+ currents of HEK293 cells stably transfected with the native rat muscle NaV1.4 clone (denoted as wild type or DEKA) and several previously characterized selectivity filter mutations of this clone: R, H, or A substitutions of K1237 denoted as DERA, DEHA, and DEAA, respectively (Favre et al., 1996; Sun et al., 1997; Huang et al., 2000). As described for NaV currents of native cells (Gage et al., 1976; Cohen et al., 1981; Salgado et al., 1986; Lönnendonker, 1989; Eickhorn et al., 1990; Makielski et al., 1993) or heterologously expressed in *Xenopus laevis* oocytes and CHO cells (Patton and Goldin, 1991; Satin et al., 1994a; Conti et al., 1996; Dumaine and Hartmann, 1996; Boccaccio et al., 1999; Moran et al., 2003; Santarelli et al., 2007a), inward Na^+ currents of NaV1.4 channels in HEK239 cells exhibit concentration-dependent block by TTX and STX that is dependent on the frequency of voltage activation.

Fig. 1 illustrates a typical protocol used to monitor use-dependent block by TTX and STX in these cells. Whole-cell NaV current was monitored before the addition of toxin by a 10-ms step depolarization to −10 mV once every 30 s from a holding potential of −120 mV to obtain the unblocked magnitude of steady-state current, I_0. Short depolarizing pulses result in fast NaV inactivation as a consequence of normal gating; however, NaV1.4 channels rapidly recover (<10 ms) from the fast inactivated state upon repolarization to −120 mV (Cummins et al., 1993; Cummins and Sigworth, 1996; Moran et al., 2003). Accordingly, there is little evidence of accumulated inactivation in the absence of toxin for the wild-type NaV1.4 channel as tested for pulse rates up to 4 Hz (Figs. 1 and 2). Upon perfusion of Na^+ bath solution containing TTX or STX while monitoring

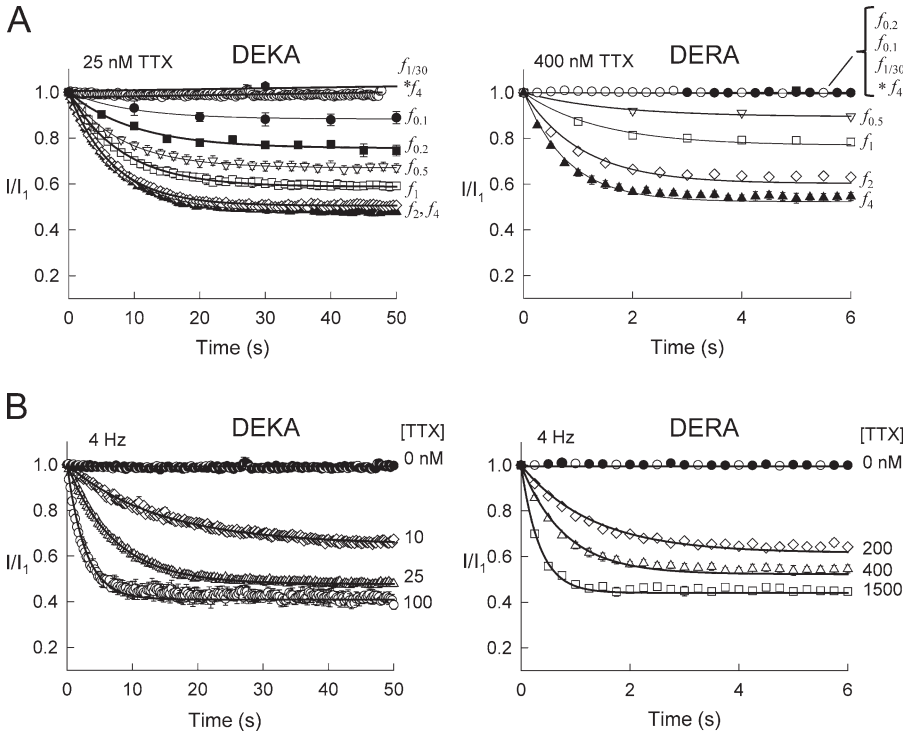

Figure 2. Time course of development of use-dependent TTX block plotted as normalized peak inward current (I/I_1) for DEKA and DERA channels. (A) Frequency dependence of development of extra block by 25 nM (left) or 400 nM TTX (right) for the two channel types in response to various stimulation rates ($f_{1/30}$, $f_{0.1}$, $f_{0.2}$, $f_{0.5}$, f_1, f_2, and f_4) of 10-ms voltage steps to −10 mV from −120 mV. Control data at 4 Hz stimulation in the absence of toxin is labeled $*f_4$. Data were collected after 55–70% tonic inhibition by TTX measured as the first pulse inward peak current, I_1. Solid lines are fits to a single exponential function. Fitted decay time constants for the DEKA channel at stimulation frequencies of 0.1, 0.2, 0.5, 1, 2, and 4 Hz are 10.4, 10.1, 8.7, 7.5, 6.6, and 7.2 s, respectively. Fitted decay time constants for DERA at stimulation frequencies of 0.5, 1, 2, and 4 Hz are 1.9, 1.4, 1.2, and 0.8 s, respectively. (B) Development of extra block at a pulse rate of 4 Hz (f_4) in the absence and presence of various concentrations of TTX in the bath solution. The fitted decay time constants for the DEKA channel at 10, 25, and 100 nM TTX are 14.2, 7.2, and 3.3 s, respectively. The fitted decay time constants for the DERA channel at 200, 400, and 1,500 nM TTX are 1.3, 0.8, and 0.3 s, respectively. Error bars indicate ±SE for 3–10 cells/patches.

whole-cell current at low frequency stimulation (1/30 Hz), Na^+ current is inhibited to a steady-state level (tonic block) that depends on toxin concentration. At the steady-state of tonic block, use dependence of TTX (Fig. 1 A) or STX (Fig. 1 B) is readily revealed by increasing or decreasing the frequency of voltage activation as shown for consecutive changes in pulse rates from four pulses/s (f_4) to one pulse every 10 s ($f_{0.1}$). Note that return to an infrequent rate (1/30 s) of voltage activation after any rapid pulse stimulation trial results in reversible relaxation of whole-cell current back to a relatively stable level of tonic block (Fig. 1).

As expected from a mutational study of the TTX/STX site (Terlau et al., 1991), mutation of Domain III selectivity filter residue K1237 renders the DERA mutant less sensitive to guanidinium toxins than the wild-type channel (~26-fold less sensitive to TTX and ~70-fold less sensitive to STX); however, this mutant retains the basic features of tonic and use-dependent toxin block as shown in Fig. 1 by enhancement of block by 400 nM TTX or 200 nM STX at high pulse rates. The dependence on toxin concentration and frequency of use-dependent block by TTX is illustrated in greater detail for wild-type and DERA channels in Fig. 2. The time course of relaxation from low frequency stimulation (1/30 s) to new steady-state level of enhanced block at higher stimulation frequency (Fig. 2 A) or as a function of increasing toxin concentration (Fig. 2 B) is well described by a single exponential, as previously described for NaV1.2 channels expressed in *Xenopus* oocytes (Conti et al., 1996). In contrast to the Na^+-selective wild-type DEKA channel ($P_K/P_{Na} = 0.08$), the DERA selectivity filter mutant does not discriminate between monovalent alkali cations such as Na^+ versus K^+ as indicated by a permeability ratio of $P_K/P_{Na} = 0.90$ measured by reversal potential (Favre et al., 1996). However, the DERA channel retains the ability to exclude Ca^{2+} from the ion conduction pathway as demonstrated by lack of inward Ca^{2+} current or positive shift toward the Ca^{2+} reversal potential (Favre et al., 1996). This implies that use-dependent block by TTX/STX does not require specific ion channel interactions that underlie discrimination of monovalent inorganic ions in the NaV channel.

The ion interaction hypothesis for use-dependent block by TTX/STX proposes that electrostatic interactions between TTX^{+1} or STX^{2+} bound to the extracellular toxin-binding site in the closed state and Na^+ or Ca^{2+} ions trapped inside the pore by the toxin result in a low binding affinity for the toxin that is relieved by inward escape of trapped inorganic ions upon transient opening of the inner activation gate during depolarization events (Salgado et al., 1986; Conti et al., 1996). To investigate whether use-dependent block by TTX is altered by Ca^{2+} permeability, we studied toxin interactions with DEHA and DEAA mutants, which are both nonselective toward monovalent inorganic cation permeation ($P_K/P_{Na} = 0.70$ for DEHA, pH 7.2; $P_K/P_{Na} = 0.87$ for DEAA) and are also significantly permeable to Ca^{2+} as demonstrated by inward Ca^{2+} current and high permeability ratios for Ca^{2+} ($P_{Ca}/P_{Na} = 3.4$ for DEHA, pH 7.2; $P_{Ca}/P_{Na} = 25$ for DEAA; Favre et al., 1996; Sun et al., 1997).

Because DEHA and DEAA mutant channels exhibit low affinity for guanidinium toxins, it is necessary to use high rates of repetitive depolarization to resolve the time course of toxin use dependence. Such behavior is similar to that previously described for certain outer pore mutations of the rat brain NaV1.2 channel (Boccaccio et al., 1999). However, high rates of repetitive depolarization of some mutant NaV channels result in enhanced cumulative inactivation even in the absence of toxin (e.g., D1717Q mutant of NaV1.2; Boccaccio et al., 1999). Fig. 3 compares the time course of cumulative inactivation for DEKA (wild type) and DEAA mutant channels activated by repetitive voltage steps to −10 mV for 1 ms from a holding potential of −120 mV delivered once

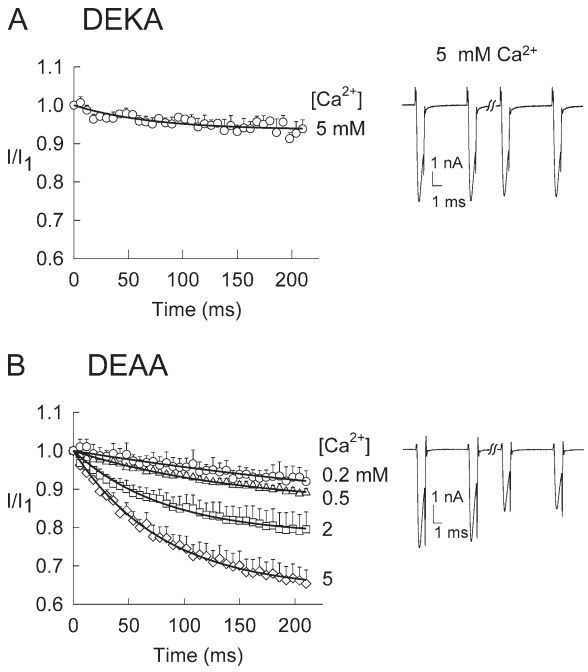

Figure 3. Ca^{2+} dependence of cumulative inactivation observed for Ca^{2+}-permeable DEAA mutant at high stimulation frequency. (A, left) Time course of normalized peak response of whole-cell currents from native DEKA channel to a 210-ms train of 1-ms pulses to −10 mV, delivered at intervals of 5 ms (167 Hz) from a holding potential of −120 mV, in the presence of external 5 mM Ca^{2+}. Peak current was reduced by ~8% at the end of 210-ms stimulation train. (right) Typical traces elicited by the first two and the last two pulses of the 210-ms stimulation train. (B, left) Time course of normalized peak response of whole-cell currents from DEAA channel to the same test protocol as in A, in the presence of 0.2, 0.5, 2, or 5 mM external Ca^{2+}. Solid lines are fits to a single exponential decay function. The fitted decay time constants of the DEAA channel for 0.2, 0.5, 2, and 5 mM Ca^{2+} are 199, 201, 100, and 86.3 ms, respectively. (right) Typical traces elicited by the first two and the last two pulses of stimulation in the presence of 5 mM Ca^{2+}. Error bars indicate ±SE for 3–10 cells/patches.

every 6 ms, equivalent to a pulse frequency of 167 Hz. The peak inward current of the wild-type DEKA channel declines by ~8% after 210 ms of 167 Hz stimulation in the presence of 5 mM extracellular Ca^{2+} (Fig. 3 A). In contrast, peak current of the DEAA mutant declines by ~35% under the same conditions (Fig. 3 B). The rate and extent of cumulative inactivation of the DEAA mutant also increase as a function of external Ca^{2+} concentration in the range of 0.2–5 mM (Fig. 3 B). Because the DEAA mutant is quite permeable to Ca^{2+} (Favre et al., 1996; Sun et al., 1997), it is possible that enhanced Ca^{2+}-dependent inactivation of this channel is related to effects on gating mediated by intracellular Ca^{2+}/calmodulin as previously described for NaV1.4 (Deschênes et al., 2002; Young and Caldwell, 2005); however, we did not further pursue the detailed basis for such Ca^{2+}-dependent cumulative inactivation in this study.

Despite the presence of significant cumulative inactivation at 167-Hz stimulation, use-dependent block of DEHA and DEAA mutants can still be observed as enhanced decay of the peak inward current in the presence of TTX relative to that in the absence of toxin (Fig. 4). As described by Boccaccio et al. (1999), the effective time course of use-dependent toxin block under such conditions of high-frequency stimulation may be extracted from the ratio of peak currents measured for the same stimulation protocol in the presence of TTX to that in the absence of TTX. This method of analysis assumes that effects of cumulative inactivation are independent of toxin use dependence, an assumption supported by considerable evidence that TTX use dependence does not involve stabilization of fast-inactivated states of gating (Patton and Goldin, 1991; Conti et al., 1996; Dumaine and Hartmann, 1996). The time course of the peak current ratio, I(+TTX)/I(−TTX), for DEHA and DEAA computed in this manner and normalized to first pulse (tonic) block (Fig. 4) has a low-affinity dependence on TTX concentration but is otherwise similar to use-dependent toxin block of the wild-type DEKA channel (Fig. 2 B). Faster kinetics of use-dependent toxin block for DEHA and DEAA in comparison with DEKA is expected for channels that exhibit low toxin-binding affinity (Boccaccio et al., 1999).

To quantitate the enhanced affinity for guanidinium toxins associated with use dependence, we constructed dose–response curves for DEKA and the three mutant channels by plotting the steady-state ratio of peak current in the presence and absence of four different toxin concentrations at low stimulation rate (1/30 Hz) and at various higher rates of voltage stimulation up to 4 Hz for DEKA and DERA and up to 167 Hz for DEHA and DEAA. Fig. 5 compares such frequency-dependent TTX dose–response curves for the four channel types. Each dose–response curve at a different stimulation frequency was fit to a one-site binding equation for dependence of unblocked current on toxin concentration, and best-fit equilibrium dissociation constants (K_d) are plotted in Fig. 6 as a function of the pulse stimulation interval. These results show that the three selectivity filter mutations of K1237 exhibit lower affinity for TTX and STX than the wild-type channel for both tonic and phasic conditions of voltage activation; however, the three mutant channels exhibit similar enhancement of toxin-blocking affinity caused by use-dependent stimulation as compared with wild type. Figs. 5 and 6 also show that the shift in the TTX dose–response curve to lower concentrations appears to approach a limiting value at high

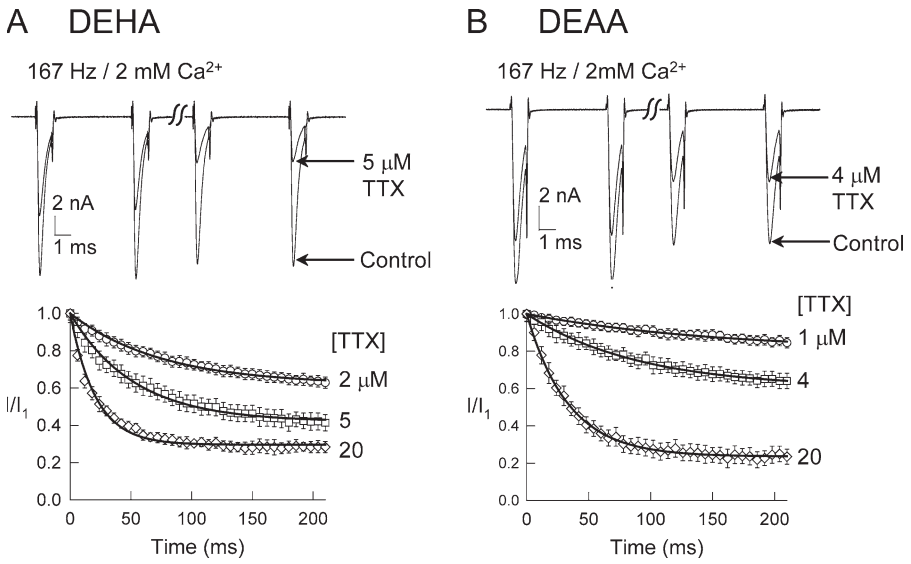

Figure 4. Time course of use-dependent block by TTX plotted as normalized current (I/I_1) for DEHA and DEAA mutant channels. (A and B, top) Superimposed current traces elicited by the first two and the last two test pulses (1 ms at −10 mV from −120 mV holding voltage) of stimulation in the absence and presence of TTX, using the same test protocol as in Fig. 3. The bath solution contained 2 mM Ca^{2+}. (bottom) Time course of extra block in response to high-frequency stimulation in the presence of various concentrations of TTX in the bath solution. Data were normalized as the ratio of peak inward current in the presence and absence of TTX as described in Materials and methods to effectively remove the background cumulative inactivation at high-frequency stimulation. Solid lines are fit to single exponential function with decay time constants for the DEHA channel at 2, 5, and 20 μM TTX of 95.2, 59.0, and 22.9 ms, respectively. The corresponding decay time constants for the DEAA channel at 1, 4, and 20 μM TTX are 180, 96.8, and 33.1 ms, respectively. Error bars indicate ±SE for 3–10 cells/patches.

stimulation frequency. Table 1 summarizes measurements of K_d^L, the toxin K_d value for conditions at the limit of low stimulation frequency (tonic) estimated by the 1/30-Hz pulse protocol and K_d^{H1}, the maximal enhancement of toxin affinity at high-frequency stimulation. K_d^{H1} was estimated by exponential fits of data in Fig. 6 to extrapolate the K_d value at zero time interval.

The mechanism of use-dependent block of NaV channels by TTX/STX may be further analyzed by the kinetic scheme of Fig. 7, which includes general features common to previous models proposed for conformational and ion interaction hypotheses (Salgado et al., 1986; Makielski et al., 1993; Satin et al., 1994a; Boccaccio et al., 1999). This model proposes that NaV channels exhibit two distinct conformations of the TTX/STX-binding site in the closed (C) state, a low-affinity closed conformation, C_L, favored at extreme negative values of membrane potential and a high-affinity closed conformation, C_H, visited on the pathway to channel opening. In structural terms, the C_L conformation is associated with the hyperpolarized configuration of the four S4 voltage sensors that stabilize the pore domain in closed state; the C_H conformation involves unspecified structural changes in the outer pore vestibule that enhance toxin-binding affinity. In principle, transition to the C_H conformation of the outer pore may involve either or both of the following kinds of structural interactions: changes in amino acid residue contacts that stabilize toxin binding or changes that weaken the repulsive interaction of toxin with trapped Na^+ and Ca^{2+} relative to C_L. Under normal conditions of voltage-dependent activation and inactivation, the open (O) state of NaV channels is very brief with a mean lifetime on the order of 1 ms at 22°C (Horn and Vandenberg, 1984). Because the time spent in the open state (O) relative to closed (C) and inactivated (I) states is a small fraction of the total recording time of standard pulse protocols (<<1%), the contribution of O states to the kinetics and equilibrium of toxin use dependence can be effectively ignored. As described in the second paragraph of Results, the use of short depolarizing test voltage pulses delivered from much longer holding intervals at −120 mV restricts the accumulation of channels in fast or slow inactivated states, and thus these states of the native channel also do not equilibrate with slow-binding toxins. (However, we note that the DEAA and DEHA channels exhibit enhanced cumulative inactivation for high-frequency stimulation.)

The kinetic scheme of Fig. 7 emphasizes equilibration of TTX/STX (Tx) binding with C_L low-affinity and C_H high-affinity closed states of the channel, with the transition from C_L to C_H or C_L·Tx to C_H·Tx favored by depolarizing voltage steps that further lead to open (O) and inactivated (I) states of the channel. Under our assay conditions, the fraction of unblocked channels at any given toxin concentration, as measured by the fraction of peak Na^+ current, corresponds to availability of the transient open unblocked state (O) reached most directly by voltage activation from the unblocked C_L and C_H closed states. Thus, in the limit of low-frequency

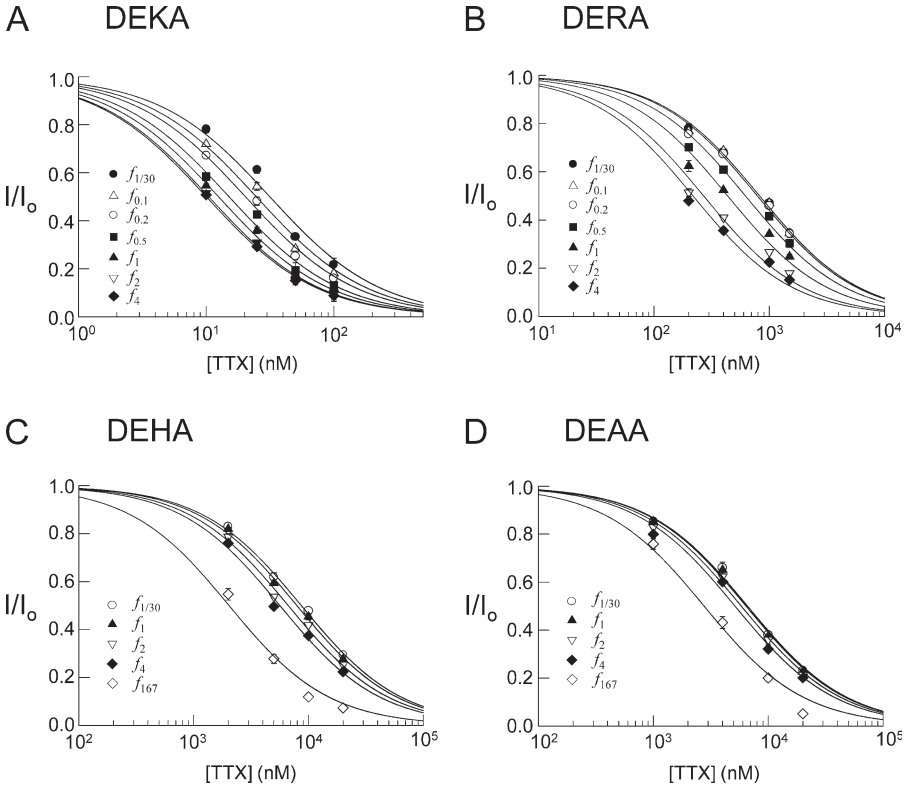

Figure 5. Concentration and frequency dependence of TTX block for native DEKA and DERA, DEHA, and DEAA mutant channels. (A–D) Data are plotted as fractional steady-state unblocked current relative to control inward peak current in the absence of toxin at each test frequency and concentration of TTX. Solid lines are best fits to $I/I_0 = K_d/(K_d + [TTX])$, assuming single-site binding. Error bars indicate ±SE for 3–10 cells/patches.

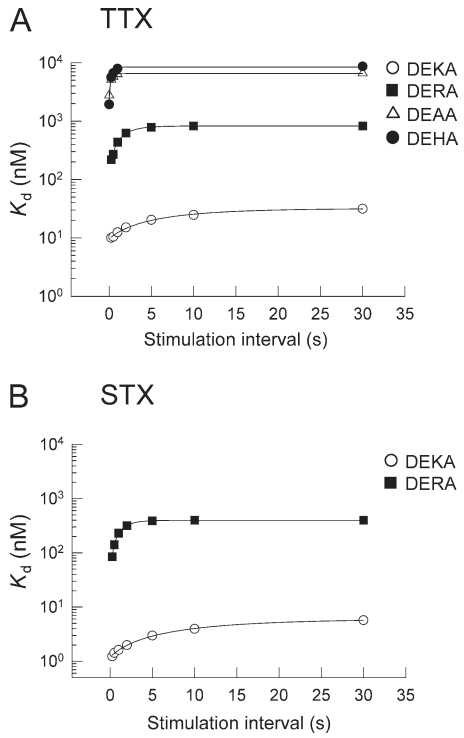

Figure 6. K_d of TTX and STX steady-state block for DEKA, DERA, DEHA, and DEAA channels plotted as a function of interpulse interval (T_i) of repetitive stimulation. (A and B) K_d was determined from the fit of dose–response curves as in Fig. 5. Solid lines are fit to an exponential rise function, $K_d(T_i) = K_d(\infty) - [K_d(\infty) - K_d(0)]\exp(-T_i/\tau)$, as discussed in the first section of Results.

stimulation (tonic), toxin dose–response curves are governed by $K_d^L = k_{off}^L/k_{on}^L$, the dissociation equilibrium constant for toxin binding to the C_L state. Similarly, in the limit of high frequency stimulation, toxin dose–response curves are expected to approach $K_d^H = k_{off}^H/k_{on}^H$, the dissociation equilibrium constant, for toxin binding to the C_H state reached from C_L by voltage depolarization. The following relationships thus define the observed equilibrium affinity and relaxation kinetics of toxin block as interpreted by the kinetic scheme of Fig. 7 (Conti et al., 1996; Moran et al., 2003):

$$\frac{I^{(t)}}{I_0} = \frac{K_d^L}{K_d^L + [Tx]} \quad (1)$$

$$\frac{I^{(s)}}{I_0} = \frac{K_d^H}{K_d^H + [Tx]} \quad (2)$$

$$F_{extra} = \frac{I^{(t)} - I^{(s)}}{I^{(t)}} = (1 - \frac{K_d^H}{K_d^L})(\frac{[Tx]}{K_d^H + [Tx]}) \quad (3)$$

$$\tau_{obs} = (\frac{1}{k_{off}^H})\frac{K_d^H}{K_d^H + [Tx]}. \quad (4)$$

Eqs. 1 and 2 define the equilibrium dissociation constants K_d^L and K_d^H for toxin (Tx) binding to the C_L and C_H states, respectively, in terms of the measured fractional unblocked current in the limit of low tonic ($I^{(t)}/I_0$) or high ($I^{(s)}/I_0$) stimulation frequency, respectively. Eq. 3 defines the maximal fraction of extra block, F_{extra}, induced by repetitive voltage stimulation and expressed as the ratio of the difference between tonic and stimulated (use dependent) levels of observed peak current, $I^{(t)} - I^{(s)}$, to the tonic level, $I^{(t)}$. At equilibrium, F_{extra} is a function of the toxin concentration, [Tx], and the two equilibrium dissociation constants for toxin binding. Eq. 4 predicts the dependence of the observed time constant for use-dependent current decay in the limit of high-frequency stimulation, τ_{obs}, as a function of toxin concentration, the equilibrium dissociation constant for toxin binding to the high-affinity state, K_d^H, and the reciprocal dissociation rate constant for toxin unbinding from this state, $1/k_{off}^H$ (Boccaccio et al., 1999).

Eqs. 2 and 4 predict that the steady-state level of unblocked current at high stimulation frequency has the

TABLE 1.

Kinetic parameters for TTX and STX

Channel	K_d^L	K_d^{H1}	K_d^{H2}	k_{off}^H	k_{on}^{H1}	k_{on}^{H2}
	nM	*nM*	*nM*	s^{-1}	$10^6/M/s$	$10^6/M/s$
TTX parameters						
DEKA	32 ± 4	9.6 ± 0.4	8.6 ± 3.6	0.031 ± 0.009	3.3 ± 0.9	3.7 ± 1.9
DERA	825 ± 36	99 ± 18	220 ± 52	0.26 ± 0.07	2.6 ± 0.9	1.2 ± 0.4
DEAA	6,600 ± 440	2,700 ± 130	2,780 ± 280	4.2 ± 0.2	1.5 ± 0.1	1.5 ± 0.2
DEHA	8,660 ± 320	1,920 ± 370	3,240 ± 260	6.5 ± 2.7	3.5 ± 1.6	2.1 ± 0.8
STX parameters						
DEKA	5.70 ± 0.39	1.19 ± 0.04	0.91 ± 0.59	0.022 ± 0.003	19 ± 3	24 ± 16
DERA	399 ± 17	17.5 ± 4.3	131 ± 40	0.73 ± 0.11	42 ± 12	5.6 ± 1.9

K_d^L was obtained from the fit of the toxin titration at low simulation frequency (1/30 Hz) to Eq. 1. K_d^{H1} was estimated from an exponential fit of K_d versus stimulation interval as in Fig. 6. K_d^{H2} and k_{off}^H were obtained from a fit to Eq. 4 of observed time constant of use-dependent enhanced block versus toxin concentration as in Fig. 8 B. k_{on}^{H1} and k_{on}^{H2} were calculated from the ratio of k_{off}^H to K_d^{H1} and K_d^{H2}, respectively. Error estimates are reported from statistics of nonlinear fits in SigmaPlot.

same dependence on toxin concentration as the time constant for use-dependent block at high frequency (e.g., Figs. 2 B and 4). Fig. 8 compares these relationships using data for use-dependent block by TTX (e.g., experiments of Figs. 2 B, 4, and 5). The results show that these expectations are reasonably well met as indicated by the comparison of similar K_d^H values obtained by the equilibrium (Fig. 8 A) or kinetic (Fig. 8 B) measurements. Fits to the data of Fig. 8 B according to Eq. 4 were used to obtain another estimate of the dissociation constant for toxin binding to the high-affinity state, K_d^{H2}.

Table 1 summarizes values of K_d^L and K_d^H obtained by the aforementioned various approaches. The wild-type and three mutant channels differ in absolute affinity for TTX and STX by up to 280-fold as indicated by their equilibrium dissociation constants but nevertheless exhibit similar use-dependent increases in affinity for both guanidinium toxins in the range of 2.4- to 23-fold for the various estimates of paired values of K_d^L/K_d^H. These results are similar to those previously reported for the effect of pore mutations at sites close to the external ring of charge in each of the four homologous domains of the rat NaV1.2 channel on TTX use dependence (Boccaccio et al., 1999). Thus, profound alterations in ionic selectivity of NaV channel permeability caused by mutation of K1257 do not abolish the structural changes that underlie the mechanism of TTX/STX use dependence. From our analysis, it is difficult to establish whether the three mutations significantly change the K_d^L/K_d^H ratio for a given toxin because the absolute value of K_d^H cannot be measured directly and is based on fits to data that involve extrapolation (e.g., Figs. 6 and 8 B) to a high-frequency limit, which is subject to various sources of error.

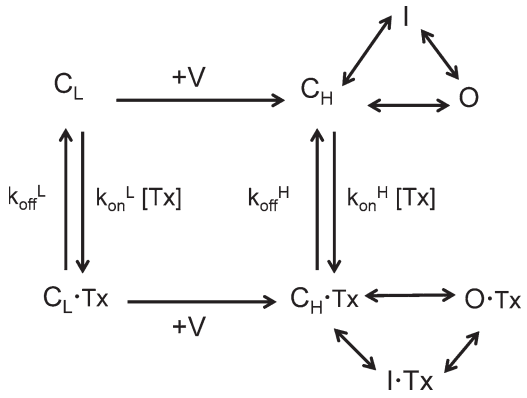

Figure 7. Hypothetical kinetic scheme for use-dependent block of NaV channels by TTX and STX. Notations: Tx, toxin; C_L, closed state with low affinity for toxin at hyperpolarized membrane potential; C_H, closed state with high affinity for toxin produced by voltage depolarization (+V) that activates movement of S4 voltage sensors en route to channel opening; O, open conducting state; I, fast-inactivated state.

The data of Fig. 8 B and Eq. 4 also allow us to estimate the dissociation rate constant of toxin unbinding from the high-affinity C_H state of the channel. Values of k_{off}^H computed by this method are summarized in Table 1 along with values of k_{on}^H calculated from the definition of the equilibrium constant, $k_{on}^H = k_{off}^H/K_d^H$. Comparison of the rate constants shows that changes in toxin affinity for the C_H state of the channel caused by mutation of K1237 are primarily reflected in changes of k_{off}^H as seen for a 200-fold increase in the TTX dissociation rate constant for DEHA relative to wild-type DEKA. Calculated k_{on}^H values typically exhibit small decreases for the three tested mutations relative to DEKA wild type. Similar changes in rate constants were observed for outer pore mutations of the rat NaV1.2 channel previously studied by Boccaccio et al. (1999), with the exception of a unique effect of one mutation in DII (E945Q) that preferentially affected the association rate constant.

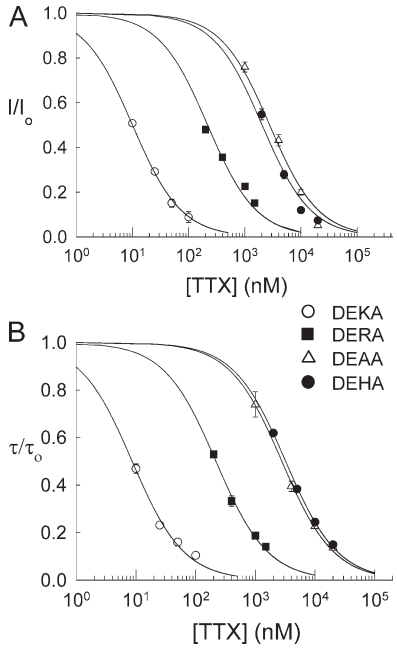

Figure 8. Comparison of TTX concentration dependence of steady-state current and relaxation time constant for use-dependent (simulated) TTX block at high frequency for DEKA and mutant channels. (A) Concentration dependence of fractional steady-state unblocked currents for DEKA, DERA, DEHA, and DEAA mutant channels for high-frequency stimulation at 4, 4, 167, and 167 Hz, respectively. Data were extracted from Fig. 5. K_d values for solid line fits to a single-site binding equation are shown in Table 1. (B) Concentration dependence of measured time constants for decay of peak current in DEKA, DERA, DEHA, and DEAA mutant channels at high-frequency stimulation rates. Time constants were obtained from experiments such as those shown in Figs. 2 and 4. For each channel, the dependence of the time constant on TTX concentration was fit to $\tau/\tau_o = K_d^H/(K_d^H + [TTX])$, shown as solid lines in the plot with τ_o and K_d^H values listed in Table 1. τ_0 is the limiting time constant of decay of peak current in the limit of low TTX concentration predicted to equal the reciprocal of the toxin dissociation rate k_{off}^H according to Eq. 4. Error bars indicate ±SE for 3–10 cells/patches.

Calcium dependence of use-dependent block

As described in the previous section, the ion interaction hypothesis for use dependence of TTX/STX block attributes the enhancement of toxin-blocking affinity to relief of an antagonistic or repulsive binding interaction between the bound cationic toxin and a Ca^{2+} or Na^{+} ion trapped between the toxin molecule and the inner gate of the channel in closed state (Conti et al., 1996). DEHA (at pH 7.2) and DEAA mutant NaV channels readily conduct Ca^{2+} current in comparison with the wild-type (DEKA) and DERA channels, which do not exhibit measurable Ca^{2+} inward current (Favre et al., 1996). The DEAA channel is also significantly less sensitive to block of inward Na^{+} current by external Ca^{2+} than the native channel as measured by the reduction in the maximal conductance (G_{max}) of the macroscopic peak current-voltage relation (Fig. 3 C of Sun et al. [1997]). Because the highly conserved K1237 selectivity filter residue of native NaV channels appears to play an important role in restricting entry of external Ca^{2+} into the ion conduction pathway, one might expect that trapped Ca^{2+} ions would have a greater probability of residing at deeper pore locations for DEHA and DEAA mutants compared with the native channel. In this scenario, the reduction of repulsion between the bound toxin and trapped Ca^{2+} could lead to a loss of toxin use dependence. However, summary results of Table 1 demonstrate that mutation of K1237 affects the intrinsic binding affinity of TTX/STX but does not eliminate enhancement of toxin affinity upon repetitive stimulation.

To further investigate the involvement of external Ca^{2+} in the mechanism of use dependence, we compared use-dependent TTX block for native NaV1.4 and the Ca^{2+}-permeable DEAA mutant in the range of 0.2–5 mM Ca^{2+}. Fig. 9 shows the time course of development of use-dependent block for 0.2, 1, and 5 mM Ca^{2+} at a stimulation frequency of 4 Hz for the DEKA channel in the presence of 25 nM TTX (Fig. 9 A) and at 167 Hz for the DEAA mutant in the presence of 4 μM TTX (Fig. 9 B). In this comparison, peak inward current for DEKA (Fig. 9 A) was normalized to the first pulse (tonic condition). DEAA current was analyzed as the normalized ratio of peak inward current in the presence and absence of TTX (Fig. 9 B) as described in the experiment of Fig. 4 to correct for toxin-independent, Ca^{2+}-dependent accumulated inactivation. The results of this comparison indicate that the Ca^{2+}-impermeable (DEKA) and Ca^{2+}-permeable (DEAA) channels exhibit a small but consistent enhancement of use-dependent block by TTX at higher external Ca^{2+}, which is similar to that previously described for the rat brain NaV1.2 channel expressed in *Xenopus* oocytes (Fig. 6 A of Conti et al., 1996). We also computed the tonic inhibition parameter, $B_i = 1 - (K_d^H/K_d^L)$, which is a measure of the maximum fractional increase in extra use-dependent block at high toxin concentration that appears as a term in Eq. 3 and is proposed to depend on external Ca^{2+} concentration according to the trapped ion mechanism for use dependence (Conti et al., 1996). We find that the B_i parameter for TTX slightly increases over the range of 0.2–5 mM Ca^{2+} (Fig. 9 C), similar to that previously described for NaV1.2 (Conti et al., 1996), but does not appear to be significantly affected by mutation of K1237 in the DEAA mutant. These results further suggest that dependence of use-dependent TTX block on external Ca^{2+} is not greatly affected by mutation of K1237 in the Ca^{2+}-permeable DEAA mutant.

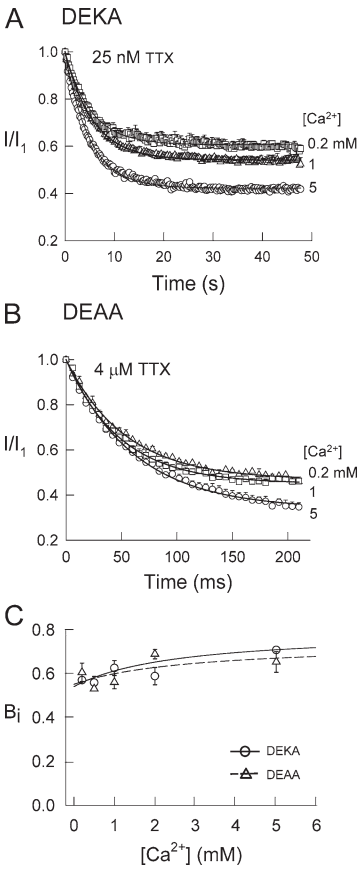

Figure 9. Effect of extracellular Ca^{2+} on use dependence of TTX block. (A) Time course of use-dependent block of the DEKA native channel by 25 nM TTX at a stimulation rate of 4 Hz (f_4) in the presence of 0.2, 1, and 5 mM external Ca^{2+}. Decay of peak inward current was fit to a single exponential function normalized to the peak inward current at the first pulse as represented by solid lines. Fitted decay time constants are 5.3, 5.9, and 5.2 for data at 0.2, 1, and 5 mM Ca^{2+}, respectively. (B) Time course of use-dependent block of the DEAA mutant channel by 4 μM TTX at a stimulation rate of 167 Hz (f_{167}) in the presence of 0.2, 1, and 5 mM external Ca^{2+}. Decay of peak inward current was fit to single exponential decay function normalized according to the current ratio in the presence and absence of TTX as described for Fig. 4. Fitted decay time constants are 47.1, 55.0, and 65.2 ms for data obtained in the presence of 0.2, 1, and 5 mM external Ca^{2+}, respectively. (C) Dependence of calculated effective tonic inhibition parameter, $B_i = 1 - (K_d^H/K_d^L)$, on extracellular Ca^{2+}. Error bars indicate ±SE for 3–10 cells/patches.

Effect of the direction of Na^+ current on use-dependent block by TTX

According to the ion interaction model for use-dependent block by TTX, development of enhanced block with repetitive depolarization is the result of equilibration of toxin binding to a new equilibrium state of higher affinity (and slower toxin dissociation rate) upon the inward release of Ca^{2+} (or Na^+) trapped in toxin-bound channels in the closed state. This model predicts that use-dependent block ought to be suppressed under conditions that favor outward ionic current because the repulsive trapped ions should be less likely to escape to the extracellular side from toxin-bound channels in the course of depolarizing voltage pulses (Conti et al., 1996). Because the preceding experiments analyzed development of use-dependent block exclusively monitored by inward Na^+ current of unblocked channels, we decided to also investigate use-dependent block as monitored by outward Na^+ current. For this purpose, we recorded Na^+ current from inside-out macropatches excised from HEK293 cells expressing wild-type NaV1.4 as previously described (Huang and Moczydlowski, 2001). Recording conditions of symmetrical 145 mM Na^+ and nominally zero divalent cations in the bath (intracellular) solution (120 mM NaF, 20 mM $NaHPO_4$, and 1.1 mM EGTA, pH 7.4) were used to enhance the magnitude of outward current and eliminate entry of Ca^{2+} or Mg^{2+} into the channel from the internal solution. Example current records and the time course of use-dependent block by 20 nM TTX in the pipette solution at 4 Hz stimulation frequency are shown in Fig. 10. Well-resolved peak Na^+ currents with a reversal potential near 0 mV were recorded from such patches. Use-dependent enhancement of TTX block was clearly present at positive voltages (50 and 100 mV) for outward current. The relaxation lifetime for development of use dependence was slightly faster at positive voltages (5.6 s at 100 mV vs. 6.5 s at −30 mV), and the fractional extra block (B_e) relative to the first pulse (tonic) block decreased by ∼24% from B_e = 0.42 at −30 mV for inward current to B_e = 0.32 for outward current at 100 mV. Thus use-dependent block clearly develops for both inward and outward Na^+ current though NaV1.4 channels. Because repetitive depolarization at high positive voltage favors loading of toxin-blocked channels with Na^+ under these conditions, the release of toxin-trapped Na^+ ought to be disfavored and use-dependent enhancement of toxin block would be expected to be diminished. Because we do observe a 24% reduction in the fraction of extra phasic block for outward current at 100 mV versus inward current at −30 mV, this may indicate a contribution of Na^+ antagonism to low toxin affinity for the tonic unstimulated condition. However, as previously discussed by Conti et al. (1996), it is difficult to predict how the ion occupancy of the channel changes in the course of repetitive depolarization and repolarization. Thus, we conclude that the quantitative effects observed in this experiment do not readily distinguish between ion interaction and conformational models of TTX use dependence.

Block of NaV1.4 by μ-conotoxin GIIIA does not exhibit use dependence

A particular class of venom peptide toxins of *Conus* marine snails known as μ-conotoxins block rat muscle NaV channels from the external side of the membrane in a competitive fashion with TTX/STX (Cruz et al., 1985; Moczydlowski et al., 1986). Although the blocking interaction of μ-conotoxin GIIIA with rat muscle NaV1.4 has been studied extensively using methods similar to those

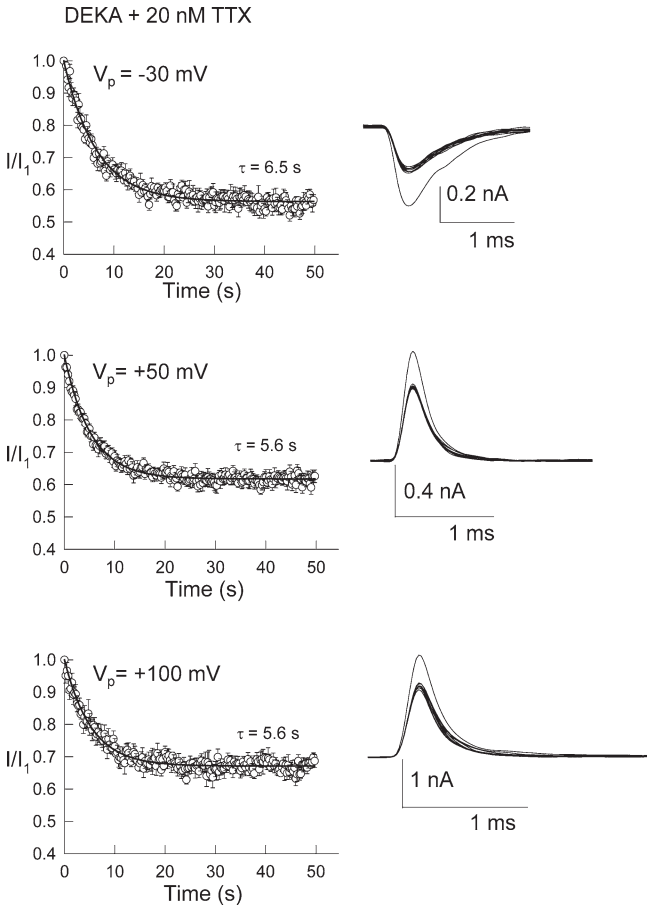

Figure 10. Voltage and current dependence of use-dependent block of DEKA channel as measured in macropatches excised from HEK293 cells under conditions of near symmetrical Na^+. 20 nM TTX was present in the extracellular pipette solution before patch formation and recording. (left) Peak current normalized to the first pulse current (I/I_1) was measured with a repetitive train of 3.25-ms pulses to −30 mV (top), 50 mV (middle), or 100 mV (bottom) from a holding potential of −120 mV at a frequency of 4 Hz (f_4 stimulation protocol). (right) Typical first and 191–200th current traces elicited by repetitive stimulations at 4 Hz using pulses of −30 (top), 50 (middle), and 100 mV (bottom). Decay of peak current was fit to a single exponential function represented by solid lines with time constants given in the figure. Error bars indicate ±SE for 3–10 cells/patches.

that reveal use dependence block by TTX/STX (e.g., Chang et al., 1998), frequency-dependent enhancement of μ-conotoxin block has not been reported, to the best of our knowledge. To confirm this relevant fact, we examined the effect of voltage pulse frequency on block of inward Na^+ currents of the NaV1.4 wild-type channel by μ-conotoxin GIIIA. Fig. 11 shows the time course of current inhibition by 80 nM μ-conotoxin GIIIA as monitored by voltage pulses delivered once every 30 s. After inhibition of the unblocked current to $I/I_0 \approx 0.6$, the stimulation pulse rate was increased to 1 Hz for 80 s and further tested at 0.5, 0.2, and 0.1 Hz before washout of the toxin by perfusion with toxin-free bath solution. During the periods of rapid stimulation, there was no evidence of enhanced time-dependent block (Fig. 11). If one assumes that μ-conotoxin exhibits use dependence similar to TTX/STX, the relationship of Eq. 4 may be used to estimate the expected time constant (τ_{obs}) of development of enhanced block. From the level of current inhibition by 80 nM toxin and rate of current recovery after washout of μ-conotoxin, we calculate an estimated K_d value of 110 nM and dissociation rate of $k_{off} = 0.0028$/s. Assuming that the affinity of the peptide toxin is enhanced threefold by repetitive voltage activation, Eq. 4 would predict a value of ~114 s for the time constant of relaxation at a high pulse frequency. With these assumptions, Eq. 3 predicts a value of $F_{extra} = 0.22$ at 80 s of monitoring at high-frequency stimulation. Thus, the experiment of Fig. 11 A with time course overlay shown in Fig. 11 B should have revealed a significant decay (~22%) of the observed current level over 80 s of monitoring at pulse rate of 1 Hz. The nearly complete lack of effect of high-frequency voltage stimulation on μ-conotoxin block confirms that the particular structural changes associated with use-dependent block by TTX/STX apparently have little effect on the kinetics of μ-conotoxin binding at its neighboring site in the external vestibule of NaV1.4.

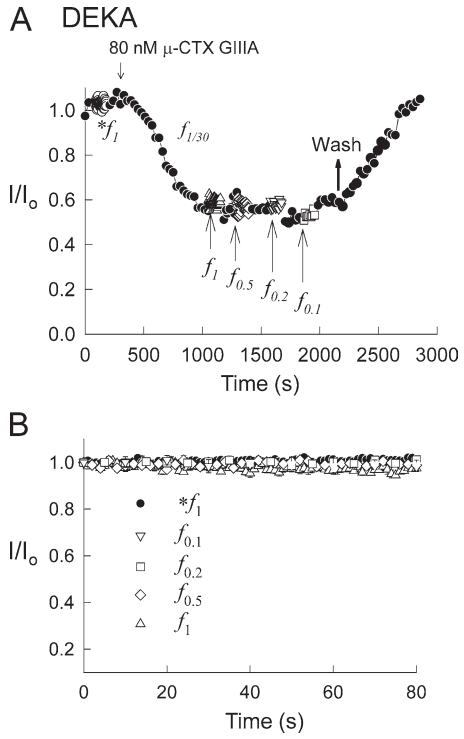

Figure 11. Absence of use dependence for external block of the rat NaV1.4 channel by μ-conotoxin GIIIA. (A) Typical wash-in and wash-out experiment for block of the DEKA native channel by 80 μM μ-CTX GIIIA. Data points are normalized inward peak whole-cell currents measured during consecutive 10-ms pulse protocols ($f_{1/30}$, $f_{0.1}$, $f_{0.2}$, $f_{0.5}$, and f_1), which are the same as those used for monitoring use dependence of TTX/STX block (e.g., Fig. 1). (B) Overlay of time course of I/I_0 data points recorded with stimulation protocols as measured in A in the absence ($*f_1$) and presence ($f_{0.1}$–f_1) of 80 μM μ-CTX GIIIA. Error bars indicate ±SE for 3–10 cells/patches.

DISCUSSION

Interaction between TTX/STX and inorganic cations

The earliest biophysical investigations of the mechanism of NaV channel block by TTX and STX suggested that these toxins target a site on the channel closely associated with binding of inorganic cations. One important piece of evidence was the fact that high-affinity binding of [^{3}H]TTX and [^{3}H]STX to excitable membranes is inhibited by low pH with a pK_a value in the range of 5.3–5.9 (Henderson et al., 1973, 1974; Reed and Raftery, 1976; Weigele and Barchi, 1978; Barchi and Weigele, 1979). The corresponding observation that TTX-sensitive Na^+ currents are blocked by external H^+ and Ca^{2+} in a weakly voltage-dependent manner (Woodhull, 1973) suggested that guanidinium toxins, H^+, and Ca^{2+} all bind to the anionic form of channel carboxyl group or groups involved in ion-selective permeation (Hille, 1975). This hypothesis was further supported by the finding that [^{3}H]TTX and [^{3}H]STX binding is competitively inhibited by monovalent alkali cations according to a high-field strength selectivity sequence ($Li^+ > Na^+ > K^+ > Rb^+ > Cs^+$) that parallels the selectivity sequence of NaV channel ionic permeability (Reed and Raftery, 1976; Weigele and Barchi, 1978; Barchi and Weigele, 1979; Doyle et al., 1993). Divalent inorganic metal cations such as Ca^{2+}, Mg^{2+}, Co^{2+}, Cd^{2+}, and Zn^{2+} also inhibit [^{3}H]STX binding to excitable membrane preparations in the millimolar range of concentration similar to their own blocking affinity (Henderson et al., 1973, 1974; Weigele and Barchi, 1978; Barchi and Weigele, 1979; Yamamoto et al., 1984; Sheets and Hanck, 1992; Doyle et al., 1993). Another important observation is the fact that mammalian cardiac NaV channels are uniquely sensitive to high-affinity block by Cd^{2+} and Zn^{2+}, which is recapitulated by similarly high-affinity inhibition of [^{3}H]STX binding to cardiac NaV channels by these same group IIB divalent metal cations (Doyle et al., 1993).

The detailed interpretation of these ion–toxin interactions requires evaluation of the relative contributions of (a) through-space electrostatics caused by negative surface potential in the vicinity of the toxin-binding site and (b) direct binding competition between TTX/STX and inorganic cations for the same microscopic chemical interactions with amino acid residues in the external vestibule of the NaV channel pore (Green and Andersen, 1986; Strichartz et al., 1986). It became possible to address this question in precise fashion by analysis of individual blocking events of TTX and STX monitored by the interruption of unitary Na^+ currents through single NaV channels inserted into planar lipid bilayers in the presence of batrachotoxin (BTX; French et al., 1984). This method required the use of BTX, which suppresses inactivation of NaV channels and shifts voltage activation to an open state probability approaching 1.0 in the voltage range more positive than approximately −80 mV. Analysis of single-channel TTX blocking events showed that the reciprocal of the biomolecular association rate of the toxin ($1/k_{on}$) is a linear function of Na^+ concentration on the external side of the channel as expected for one-to-one binding competition between TTX^{1+} and Na^+ according to: $1/k_{on} = (1/k_{on}^0)\{1 + [Na^+]/K_{Na}\}$, where k_{on}^0 is the bimolecular rate constant in the limit of zero Na^+ and K_{Na} is the Na^+ dissociation equilibrium constant (Moczydlowski et al., 1984; Green et al., 1987). However, k_{on} for STX^{2+} exhibited a steeper dependence on $[Na^+]$ than TTX^{1+}, as would be expected for a valence-dependent through-space electrostatic effect of negative surface charge (Green et al., 1987). Application of Gouy–Chapman theory to such data showed that binding of TTX^{1+} and STX^{2+} to various NaV channels is subject to enhancement by negative surface potential that originates from a surface charge density at the TTX/STX binding site in the range of 1e-/300 $Å^2$ to 1e-/450 $Å^2$ (Green et al., 1987; Ravindran and Moczydlowski, 1989). Importantly, the dissociation rate constant (k_{off}) for both TTX and STX is rather insensitive to Na^+ over a wide range of $[Na^+]$ and ionic strength (Moczydlowski et al., 1984; Green et al., 1987; Ravindran and Moczydlowski, 1989). This behavior is strong evidence that any Na^+ ions that may be trapped or bound simultaneously with TTX/STX exert little repulsive influence on the dissociation rate of guanidinium toxins, at least for the BTX-modified open state. In summary, planar bilayer experiments showed that TTX/STX is physically excluded from binding to the NaV channel by mutual competition with at least one Na^+ ion and binding of these charged toxins is also subject to the attractive electrostatic influence of a negative surface potential.

Similar results were found for the interaction of divalent metal cations and the blocking reaction of TTX/STX as studied with BTX-modified open NaV channels of mammalian brain. Ba^{2+}, Ca^{2+}, and Zn^{2+} were all found to strongly decrease the observed bimolecular association rate of TTX and STX with little effect on the toxin dissociation rate constant (Worley et al., 1986; Green et al., 1987). The unique sensitivity of mammalian cardiac NaV channels to high-affinity block by Zn^{2+} (Ravindran et al., 1991) enabled the binding interaction between STX^{2+} and Zn^{2+} to be examined at the single-channel level using Zn^{2+} concentrations <200 μM, an ionic strength at which changes in surface potential by charge screening can be largely excluded. The results clearly showed that STX^{2+} competes with Zn^{2+} for binding to the cardiac NaV channel in a mutually exclusive fashion with respective intrinsic K_d values for these two ligands of ∼30 nM for STX and ∼20 μM for Zn^{2+} at the conditions of the assay (Schild and Moczydlowski, 1991).

Mutational studies subsequently showed that the unique high sensitivity to rat heart NaV1.5 channels to block by thiophilic group IIB divalent cations such as Zn^{2+} and Cd^{2+} and the relative low affinity for TTX/STX for this NaV gene isoform is caused by the presence of a sulfhydryl-containing Cys374 residue in the cardiac channel, which corresponds to an aromatic Tyr401 residue in rat muscle NaV1.4 and Phe385 in rat brain NaV1.2 (Backx et al., 1992; Heinemann et al., 1992a; Satin et al., 1992; Favre et al., 1995). Many complementary studies concerning the identification of amino acid residues in the outer pore region of NaV channels that participate in TTX/STX binding, divalent cation block, and ionic selectivity for permeation have been conducted (e.g., Terlau et al., 1991; Heinemann et al., 1992a; Schlief et al., 1996). Although an exact three-dimensional structure of TTX/STX bound to an actual NaV channel is still lacking, these results provide a firm rationale for investigating the possible relationship between use-dependent block by TTX/STX and ion occupancy of the NaV channel pore.

Dependence of use-dependent block by TTX/STX on NaV channel gating

The first detailed analyses of phasic block by TTX based on voltage-clamp recording of low-TTX-affinity Na^+ current of mammalian heart cells led to the suggestion that toxin-blocked channels exhibit altered gating behavior involving slow transitions between toxin-occupied closed and inactivated states (Cohen et al., 1981). This interpretation is similar to the modulated receptor model used to explain the kinetics of use-dependent block of NaV channels by local anesthetics (Hille, 1977). However, access and escape of local anesthetic drugs can be expected to depend on transitions to or from closed or inactivated states that control movement of the internal gate that physically restricts escape of ions and drugs that bind within the channel pore. In contrast, it is hard to envision how access to the external TTX-binding site can depend on such gating. Another important finding was the fact that the

development of extra block in the presence of preequilibrated TTX could be observed in response to a single brief voltage pulse (Cohen et al., 1981). This behavior is analogous to a kind of fast, transient molecular memory, as if the toxin-bound channel remembers the experience of being stimulated with voltage for <1 ms and responds by strengthening its association with the toxin for several seconds, then forgets that the stimulus ever occurred over the course of the next minute.

Similar voltage-clamp experiments were performed with high-toxin-affinity NaV channels of frog myelinated nerve where the kinetics of development and decay of extra block by both TTX and STX were also tracked by a two-pulse protocol (Lönnendonker, 1989). A key observation of these experiments also previously noted by Salgado et al. (1986) was the fact that an extremely brief depolarizing voltage pulse as short as 0.2 ms in duration is sufficient to trigger maximal extra block. Because this depolarization stimulus is shorter than the time at which macroscopic Na^+ current peaks in this nerve preparation at ~0.5 ms, it suggests that brief stimulation of channel activation is all that is required to trigger extra block; inactivation gating of the channel does not appear to be involved. Lönnendonker (1989) concluded that use-dependent TTX/STX block appears to involve "a fast affinity increase of toxin receptors of Na^+ channels triggered by Na^+ activation followed by slow toxin binding to channels and relaxation of the receptor affinity."

The use of cloned NaV channels to investigate the role of channel gating in use-dependent block by TTX was introduced using the rat neuronal NaV1.2 channel expressed in *Xenopus* oocytes (Patton and Goldin, 1991). Use-dependent TTX block in this preparation was shown to be dependent on holding potential such that maximal approximately threefold enhancement of TTX affinity is observed at holding voltages more negative than approximately −100 mV. In contrast, a holding voltage more positive than −60 mV results in the loss of phasic enhancement of toxin affinity with a concomitant increase in tonic affinity for TTX. Increasing the duration of conditioning pulses >3 ms did not affect the fraction of extra block in agreement with Lönnendonker (1989). A mutant with impaired fast inactivation also did not affect the degree or kinetics of extra block (Patton and Goldin, 1991). In contrast, a different NaV1.2 mutation that shifted the voltage dependence of activation by about 20 mV similarly shifted the voltage dependence of the pulse amplitude used to trigger use-dependent block. The requirement for a holding voltage more negative than −80 mV and the dependence on pulse voltage that mimics the voltage dependence of NaV channel activation was confirmed for NaV1.2 expressed in *Xenopus* oocytes by Conti et al. (1996). The gating study of Patton and Goldin (1991) thus supports the view that a closed conformational state of the channel primed for activation favors the development of use-dependent enhancement of TTX block on the kinetic pathway to opening of the channel, but actual opening of the channel is not necessarily required. In contrast, the inactivated state appears to exhibit an enhanced steady-state TTX-binding affinity but lacks the capability to develop extra block from that state (Patton and Goldin, 1991). A key difference in interpretation of these results with respect to the conformational and trapped ion models concerns the hypothesis that voltage pulses that trigger movement of the S4 voltage sensors leading to channel activation also lead to clearing of trapped ions (Na^+ and Ca^{2+}) that inhibit toxin binding via inward movement of these ions even at very low opening probability (Conti et al., 1996).

Further evidence against the involvement of fast inactivation gating is the fact that removal of fast inactivation by mutation of IFM→QQQ in the DIII–DIV interdomain linker of the human cardiac NaV channel does not reduce the fractional enhancement of extra block by TTX, nor does it affect the kinetics of development and recovery of postrepolarization block as monitored by the two-pulse protocol (Dumaine and Hartmann, 1996). In contrast, a pharmacological method of removing fast inactivation with the use of BTX eliminates use dependence of block by TTX as observed for native rat cardiac NaV channels recorded in primary cultured ventricular cells (Huang et al., 1987). BTX is known to alter NaV channel ionic selectivity and unmask voltage-dependent kinetics of TTX/STX binding to the open state of the BTX-modified channel (French et al., 1984; Moczydlowski et al., 1984; Strichartz et al., 1986; Green et al., 1987). Such voltage-dependent binding to the native open state cannot be measured for normally inactivating NaV channels because the brief channel openings do not allow binding equilibration of the toxins to this state. A similar, but shallower voltage dependence of TTX/STX binding has also been observed for the closed state of normally inactivating NaV channels at hyperpolarized holding potentials (Satin et al., 1994b). These observations reinforce the idea that normal fast inactivation gating is not required for TTX/STX use dependence. However, changes in gating and ion permeation induced by BTX apparently alter the subtle conformational or ionic interactions that underlie TTX/STX use dependence.

Evidence relevant to the trapped cation model for use-dependent block by TTX/STX

The trapped ion model was first introduced as an ingenious hypothesis to describe use-dependent block of invertebrate Na^+ channels by STX as elegantly studied using perfused giant axons of *Procambarus clarkii* crayfish (Salgado et al., 1986). The idea that monovalent (Na^+) or divalent cations (Ca^{2+}) can be simultaneously trapped inside the channel pore with TTX or STX

bound in the outer vestibule is not inconsistent with current models of NaV channel structure (Fozzard and Lipkind, 2010; Payandeh et al., 2011). The evidence for a competitive binding interaction between inorganic cations and TTX/STX cited in the first section of this Discussion implies that there is at least one overlapping site where the binding of these two classes of ligands is mutually exclusive. However, this does not obviate the possibility that inorganic cations may be also bound at other sites simultaneously with a toxin molecule, perhaps at deeper locations in the selectivity filter or central cavity, when the toxin is bound to the closed channel. One question in evaluating this mechanism is whether the hypothetical repulsive interaction between Na^+/Ca^{2+} and TTX^{1+}/STX^{2+} would be strong enough to reduce the equilibrium affinity for the toxin by a factor of 3 or more, the difference in toxin affinity between tonic and phasic extremes of voltage stimulation. Furthermore, assuming that simultaneous binding of trapped inorganic cations and guanidinium toxin does occur, another question that would need to be explained is: Why do the sequestered inorganic cations not simply move deeper into the channel at negative voltage, if there is substantial repulsion between trapped ions and the toxin? Significant movement of trapped cations to sites located closer to or within the internal central cavity capped off by the closed internal gate would be favored by relief of the local electrostatic repulsion. The trapped ion mechanism of use dependence seems to require special structural features that position the trapped ions and bound toxin in close proximity in the closed state to experience repulsion, but also allow the ions to readily move inward with the onset of a brief voltage pulse.

In support of the trapped ion model, increased external $[Ca^{2+}]$ generally decreases the resting affinity for toxin and increases the maximal fraction of use-dependent block (Fig. 9; Salgado et al., 1986; Lönnendonker, 1991; Conti et al., 1996; Moran et al., 2003). However, the Ca^{2+} dependence of toxin use dependence may also be explained by Ca^{2+}-dependent shifts in gating parameters (Hille et al., 1975) or toxin binding (Green et al., 1987) caused by changes in local surface potential. Also relevant is the fact that TTX/STX use dependence is not abolished by low or zero concentration of external divalent cations (Satin et al., 1994a; Conti et al., 1996). According to the trapped ion model, this is explained by the notion that use dependence is also mediated by a repulsive toxin interaction with Na^+ ion in the absence of Ca^{2+} (Conti et al., 1996; Moran et al., 2003). However, in an experiment in which external $[Na^+]$ was reduced fivefold from 96 to 19 mM with Na^+ replacement by external $Tris^+$, there was no effect on the time course or extent of extra block by TTX with repetitive stimulation (Patton and Goldin, 1991).

These considerations and uncertainties led us to examine the effect of changes in monovalent and divalent inorganic cation selectivity on TTX/STX use dependence by experiments presented in this paper. Our hypothesis was that TTX/STX use dependence would be reduced or lost if ion coordination and selectivity were altered by mutation of the selectivity filter. Our major finding is that elimination of either Na^+/K^+ selectivity with the DERA mutation or enhancement of Ca^{2+} permeability with the DEHA and DEAA mutations does not abolish or systematically change the magnitude of TTX/STX use dependence as indicated by the estimated change in toxin affinity between tonic and frequency-dependent conditions of voltage stimulation (Table 1). The tested mutations of the K1237 selectivity filter residue change the absolute affinity of TTX and STX by up to 270-fold, but the three mutant channels retain the basic feature of use-dependent enhancement of toxin block with kinetics that reflect toxin affinity. Thus, our results are similar to those of other studies that previously explored the effect of different mutations of the outer pore region on TTX/STX use dependence (Satin et al., 1994a; Boccaccio et al., 1999; Santarelli et al., 2007a).

We also observed that the DEAA mutation (and to a lesser extent DEHA) exhibits enhanced Ca^{2+}-dependent cumulative fast inactivation (Fig. 3) that is likely to be related to enhanced permeation of Ca^{2+} (Favre et al., 1996). However, the DEAA and DEHA mutations do not appear to affect the Ca^{2+} dependence of use dependence block by TTX (Fig. 9). Additionally, we found that the kinetics of use-dependent block by TTX does not strongly depend on the direction of Na^+ current as measured in inside-out macropatches (Fig. 10). Because outward current polarity disfavors the escape of trapped ions from the channel in the toxin-bound closed state, this result weighs against the trapped ion hypothesis (but see additional arguments in Conti et al. [1996]).

Findings similar to our results have also been reported for unnatural amino acid mutations of the Tyr401 residue of rat NaV1.4 (Santarelli et al., 2007a). As described in the last paragraph of the first section of this Discussion, Tyr401 is a residue that is important for NaV channel isoform differences in affinity for TTX/STX, with toxin-sensitive NaV channels having aromatic Tyr or Phe at this location and replacement by Cys for the toxin-insensitive cardiac NaV1.5 channel. Consecutive addition of up to three fluorine atoms to the ring of Phe residues reduces the negative electrostatic character of the planar π-orbital surfaces of the aromatic ring. Such chemical mutations are predicted to quench possible cation–π interactions between guanidinium groups of the TTX/STX and Phe401. Santarelli et al. (2007a) used this method to show that a cation–π interaction is indeed the likely basis for high TTX/STX

affinity in toxin-sensitive NaV channels. Phe fluorination mutations were found to decrease the affinity for TTX block in linear proportion to the number of fluorine atoms as expected for a cation–π interaction (Santarelli et al., 2007a). However, all of the tested mutations in an affinity range accessible to the kinetics of use dependence were found to exhibit a typical approximately threefold decrease of the K_d for TTX from tonic to phasic conditions of voltage stimulation. Interestingly, the Tyr401 residue also appears to interact electrostatically with external Ca^{2+} because the apparent equilibrium blocking dissociation constant for external Ca^{2+} is increased from 21 to 59 mM with consecutive addition of up to three fluorine atoms to Phe401 (Santarelli et al., 2007b). Because both Ca^{2+} and TTX^{1+} directly interact with Tyr401, these experiments also show that perturbation of Ca^{2+} binding in the external vestibule near the selectivity filter does not affect toxin use dependence. Thus, it currently appears that mutational attempts to correlate use dependence of TTX/STX with Ca^{2+} binding in the external vestibule of NaV channel fail to support the trapped cation hypothesis.

Conformational changes of the selectivity filter region coupled to NaV channel gating explain use dependence of TTX/STX block

Since the phenomenon of use-dependent block of TTX/STX was first discovered and well characterized (Cohen et al., 1981), much new information has been learned about NaV channel gating. In particular, there is considerable evidence of mutations in the outer pore of NaV channels (Balser et al., 1996; Bénitah et al., 1999; Todt et al., 1999; Hilber et al., 2005; Xiong et al., 2006; Zarrabi et al., 2010) and manipulations of external permeant ions (Townsend and Horn, 1997) that affect slow inactivation gating. Slow inactivation of NaV channels occurs in response to long-duration depolarization and is thought to resemble C-type inactivation in K^+ channels, which involves ion-dependent conformational changes in the selectivity filter region (López-Barneo et al., 1993; Liu et al., 1996; Cordero-Morales et al., 2006; Cuello et al., 2010).

Recently, direct coupling between electromechanical movement of the DIV voltage sensor domain (comprised of one S1–S4 structural element in homologous Domain IV) and the outer pore domain of NaV1.4 (formed by four S5-P-S6 segments) has been discovered (Capes et al., 2012). These findings have important implications for the mechanism of guanidinium toxin use dependence. The work of Capes et al. (2012) revealed that TTX preferentially inhibits gating pore currents mediated by the charge-neutralized D(IV)-S4 mutant voltage sensor element in contrast to negligible effects of TTX on gating pore current of the other three voltage sensor domains. TTX also inhibits actual off-gating current of the native NaV1.4 channel (Capes et al., 2012), similar to previously reported inhibition by TTX/STX of NaV channel gating currents of crayfish axons (Heggeness and Starkus, 1986). These new observations establish a coupled interaction between TTX/STX binding to the selectivity filter region and voltage-dependent movement of the DIV voltage sensor required for NaV channel activation (Capes et al., 2012). Such a mechanical coupling between DIV-S4 and binding of STX/TTX to the outer filter region would be the kind of interaction that is consistent with characterized behavior of use-dependent block by TTX/STX. In this scenario, the minimal steps in triggering use dependence would involve brief depolarization from hyperpolarized membrane voltage that mechanically transmits a conformational change initiated by the outward movement of DIV-S4 to the toxin-binding site in the pore domain. Because the DIV-S4 segment is physically attached to the pore domain via the internal S4–S5 linker region and the internal side of the S5 helix, conformational changes transmitted to the outer pore would also have to involve conformational changes of the internal pore region. In accord with this expectation, interactions between external and internal residues of the pore domain of NaV1.4 have been implicated in the mechanism of ultra-slow inactivation (Zarrabi et al., 2010).

In contrast to the cited interaction between TTX binding and the DIV voltage sensor domain, μ-conotoxin peptide, which also blocks the NaV1.4 channel by binding within the external vestibule, only inhibits DIV gating pore current of a charge-neutralized mutant very weakly and has no effect on actual gating current of the native channel (Capes et al., 2012). The differential effect of the two classes of pore toxins can be explained by the fact that guanidinium toxins such as TTX/STX bind more deeply in the NaV channel pore in closer proximity to the DEKA selectivity filter residues than μ-conotoxin, which interacts with more superficially located vestibule residues (Hui et al., 2002; Li et al., 2003) and does not compete with Na^+ for binding (Li et al., 2003). Certain versions of μ-conotoxin (KIIIA) that produce incomplete block or current subconductance events can actually occupy the outer vestibule simultaneously with TTX or STX bound close to the filter (Zhang et al., 2009, 2010). These facts may help to explain the present observations that TTX and STX exhibit use-dependent block (Fig. 1) but μ-conotoxin does not (Fig. 11). If the conformational changes transmitted between the DIV voltage sensor and the pore domain are localized to the deeper regions of the outer vestibule closer to the selectivity filter, then TTX/STX binding would be more sensitive to these changes than μ-conotoxin.

Summary and conclusions

We studied three different ion-selectivity mutants of the key K1237 residue that determines Na^+/K^+ discrimination

and Ca^{2+} permeability of NaV channels to investigate the possible role of interactions with inorganic cations in the mechanism of TTX/STX use-dependent block. These selectivity filter mutations strongly affect the intrinsic binding affinity and kinetics of guanidinium toxins but do not eliminate the characteristic enhancement of toxin affinity known as use dependence that arises from brief repetitive voltage stimulation for all tested NaV channels. Mounting evidence suggests that the mechanism of TTX/STX use dependence involves conformational coupling of the external toxin-binding site with the voltage-sensing domains, particularly DIV-S4. An unsolved problem concerns the actual conformational changes of the TTX/STX-binding site responsible for the use-dependent enhancement of toxin-binding affinity. None of the mutations of the toxin-binding site that have been examined so far eliminate use dependence. One possibility is that subtle conformational changes of many residues contribute to the overall enhancement of toxin-binding affinity by small additive increments of free energy. Such a mechanism would be analogous to the induced-fit model of enzyme–substrate interaction (Koshland, 1958). For an induced-fit mechanism applied to the NaV channel, the mean conformation of the TTX/STX-binding site may be poised for low affinity at the hyperpolarized state of the voltage-sensing apparatus. This may be caused by constraints on the protein structure optimized for fast channel opening and ion conduction upon activation. Subtle movement of the voltage sensors preceding channel opening driven by brief repetitive depolarization may be sufficient to relax the conformation of the toxin-binding site in the closed state to favorably conform to the bound toxin structure and enhance its equilibrium binding affinity. Conformational changes that enhance toxin-binding affinity may also favor the process of slow inactivation that normally acts as a stabilizing protection against hyperexcitation. In support of this concept, induced-fit structural rearrangement of preexisting conformations of both peptide toxin ligands and K^+ channel proteins has been observed to occur upon peptide–channel association by solid-state nuclear magnetic resonance (Lange et al., 2006) and molecular dynamics simulations (Huang et al., 2005). A more refined understanding of such toxin use dependence for the NaV channel may facilitate development of a new class of synthetic toxin-based drug ligands that target the suppression of electrical signaling in conditions of hyperexcitability such as chronic pain.

We would like to thank Dr. Isabelle Favre for expert molecular biology and creation of mutant versions of NaV1.4 expressed in HEK293 cells.

This work was previously supported by a grant from the National Institute of General Medical Sciences (GM-51172) and currently by an Early Career Laboratory Directed Research and Development award from Sandia National Laboratories to E.G. Moczydlowski. Sandia National Laboratories is a multiprogram laboratory managed and operated by Sandia Corporation, a wholly owned subsidiary of Lockheed Martin Corporation, for the U.S. Department of Energy's National Nuclear Security Administration under contract DE-AC04-94AL85000.

Kenton J. Swartz served as editor.

Submitted: 28 June 2012
Accepted: 31 August 2012

REFERENCES

Ahern, C.A., A.L. Eastwood, D.A. Dougherty, and R. Horn. 2008a. Electrostatic contributions of aromatic residues in the local anesthetic receptor of voltage-gated sodium channels. *Circ. Res.* 102: 86–94. http://dx.doi.org/10.1161/CIRCRESAHA.107.160663

Ahern, C.A., A.L. Eastwood, D.A. Dougherty, and R. Horn. 2008b. New insights into the therapeutic inhibition of voltage-gated sodium channels. *Channels (Austin).* 2:1–3. http://dx.doi.org/10.4161/chan.2.1.6007

Backx, P.H., D.T. Yue, J.H. Lawrence, E. Marban, and G.F. Tomaselli. 1992. Molecular localization of an ion-binding site within the pore of mammalian sodium channels. *Science.* 257:248–251. http://dx.doi.org/10.1126/science.1321496

Baer, M., P.M. Best, and H. Reuter. 1976. Voltage-dependent action of tetrodotoxin in mammalian cardiac muscle. *Nature.* 263:344–345. http://dx.doi.org/10.1038/263344a0

Balser, J.R., H.B. Nuss, N. Chiamvimonvat, M.T. Pérez-García, E. Marban, and G.F. Tomaselli. 1996. External pore residue mediates slow inactivation in μ 1 rat skeletal muscle sodium channels. *J. Physiol.* 494:431–442.

Barchi, R.L., and J.B. Weigele. 1979. Characteristics of saxitoxin binding to the sodium channel of sarcolemma isolated from rat skeletal muscle. *J. Physiol.* 295:383–396.

Bénitah, J.-P., Z. Chen, J.R. Balser, G.F. Tomaselli, and E. Marbán. 1999. Molecular dynamics of the sodium channel pore vary with gating: interactions between P-segment motions and inactivation. *J. Neurosci.* 19:1577–1585.

Boccaccio, A., O. Moran, K. Imoto, and F. Conti. 1999. Tonic and phasic tetrodotoxin block of sodium channels with point mutations in the outer pore region. *Biophys. J.* 77:229–240. http://dx.doi.org/10.1016/S0006-3495(99)76884-0

Capes, D.L., M. Arcisio-Miranda, B.W. Jarecki, R.J. French, and B. Chanda. 2012. Gating transitions in the selectivity filter region of a sodium channel are coupled to the domain IV voltage sensor. *Proc. Natl. Acad. Sci. USA.* 109:2648–2653. http://dx.doi.org/10.1073/pnas.1115575109

Cervenka, R., T. Zarrabi, P. Lukacs, and H. Todt. 2010. The outer vestibule of the Na^+ channel-toxin receptor and modulator of permeation as well as gating. *Mar Drugs.* 8:1373–1393. http://dx.doi.org/10.3390/md8041373

Chang, N.S., R.J. French, G.M. Lipkind, H.A. Fozzard, and S. Dudley Jr. 1998. Predominant interactions between μ-conotoxin Arg-13 and the skeletal muscle Na^+ channel localized by mutant cycle analysis. *Biochemistry.* 37:4407–4419. http://dx.doi.org/10.1021/bi9724927

Choudhary, G., L. Shang, X. Li, and S.C. Dudley Jr. 2002. Energetic localization of saxitoxin in its channel binding site. *Biophys. J.* 83:912–919. http://dx.doi.org/10.1016/S0006-3495(02)75217-X

Cohen, C.J., B.P. Bean, T.J. Colatsky, and R.W. Tsien. 1981. Tetrodotoxin block of sodium channels in rabbit Purkinje fibers. Interactions between toxin binding and channel gating. *J. Gen. Physiol.* 78:383–411. http://dx.doi.org/10.1085/jgp.78.4.383

Conti, F., A. Gheri, M. Pusch, and O. Moran. 1996. Use dependence of tetrodotoxin block of sodium channels: a revival of the

trapped-ion mechanism. *Biophys. J.* 71:1295–1312. http://dx.doi.org/10.1016/S0006-3495(96)79330-X

Cordero-Morales, J.F., L.G. Cuello, and E. Perozo. 2006. Voltage-dependent gating at the KcsA selectivity filter. *Nat. Struct. Mol. Biol.* 13:319–322. http://dx.doi.org/10.1038/nsmb1070

Cruz, L.J., W.R. Gray, B.M. Olivera, R.D. Zeikus, L. Kerr, D. Yoshikami, and E. Moczydlowski. 1985. *Conus geographus* toxins that discriminate between neuronal and muscle sodium channels. *J. Biol. Chem.* 260:9280–9288.

Cuello, L.G., V. Jogini, D.M. Cortes, and E. Perozo. 2010. Structural mechanism of C-type inactivation in K(+) channels. *Nature.* 466:203–208. http://dx.doi.org/10.1038/nature09153

Cummins, T.R., and F.J. Sigworth. 1996. Impaired slow inactivation in mutant sodium channels. *Biophys. J.* 71:227–236. http://dx.doi.org/10.1016/S0006-3495(96)79219-6

Cummins, T.R., J. Zhou, F.J. Sigworth, C. Ukomadu, M. Stephan, L.J. Ptácek, and W.S. Agnew. 1993. Functional consequences of a Na^+ channel mutation causing hyperkalemic periodic paralysis. *Neuron.* 10:667–678. http://dx.doi.org/10.1016/0896-6273(93)90168-Q

Deschênes, I., N. Neyroud, D. DiSilvestre, E. Marbán, D.T. Yue, and G.F. Tomaselli. 2002. Isoform-specific modulation of voltage-gated Na^+ channels by calmodulin. *Circ. Res.* 90:E49–E57. http://dx.doi.org/10.1161/01.RES.0000012502.92751.E6

Doyle, D.D., Y. Guo, S.L. Lustig, J. Satin, R.B. Rogart, and H.A. Fozzard. 1993. Divalent cation competition with [^{3}H]saxitoxin binding to tetrodotoxin-resistant and -sensitive sodium channels. A two-site structural model of ion/toxin interaction. *J. Gen. Physiol.* 101:153–182. http://dx.doi.org/10.1085/jgp.101.2.153

Dumaine, R., and H.A. Hartmann. 1996. Two conformational states involved in the use-dependent TTX blockade of human cardiac Na^+ channel. *Am. J. Physiol.* 270:H2029–H2037.

Eickhorn, R., J. Weirich, D. Hornung, and H. Antoni. 1990. Use dependence of sodium current inhibition by tetrodotoxin in rat cardiac muscle: influence of channel state. *Pflugers Arch.* 416:398–405. http://dx.doi.org/10.1007/BF00370746

Favre, I., E. Moczydlowski, and L. Schild. 1995. Specificity for block by saxitoxin and divalent cations at a residue which determines sensitivity of sodium channel subtypes to guanidinium toxins. *J. Gen. Physiol.* 106:203–229. http://dx.doi.org/10.1085/jgp.106.2.203

Favre, I., E. Moczydlowski, and L. Schild. 1996. On the structural basis for ionic selectivity among Na^+, K^+, and Ca^{2+} in the voltage-gated sodium channel. *Biophys. J.* 71:3110–3125. http://dx.doi.org/10.1016/S0006-3495(96)79505-X

Fozzard, H.A., and G.M. Lipkind. 2010. The tetrodotoxin binding site is within the outer vestibule of the sodium channel. *Mar Drugs.* 8:219–234. http://dx.doi.org/10.3390/md8020219

Fozzard, H.A., M.F. Sheets, and D.A. Hanck. 2011. The sodium channel as a target for local anesthetic drugs. *Front Pharmacol.* 2:68. http://dx.doi.org/10.3389/fphar.2011.00068

French, R.J., J.F. Worley III, and B.K. Krueger. 1984. Voltage-dependent block by saxitoxin of sodium channels incorporated into planar lipid bilayers. *Biophys. J.* 45:301–310. http://dx.doi.org/10.1016/S0006-3495(84)84156-9

Gage, P.W., J.W. Moore, and M. Westerfield. 1976. An octopus toxin, maculotoxin, selectively blocks sodium current in squid axons. *J. Physiol.* 259:427–443.

Goldin, A.L. 2003. Mechanisms of sodium channel inactivation. *Curr. Opin. Neurobiol.* 13:284–290. http://dx.doi.org/10.1016/S0959-4388(03)00065-5

Green, W.N., and O.S. Andersen. 1986. Surface charges near the guanidinium neurotoxin binding site. *Ann. N. Y. Acad. Sci.* 479:306–312. http://dx.doi.org/10.1111/j.1749-6632.1986.tb15577.x

Green, W.N., L.B. Weiss, and O.S. Andersen. 1987. Batrachotoxin-modified sodium channels in planar lipid bilayers. Characterization of saxitoxin- and tetrodotoxin-induced channel closures. *J. Gen. Physiol.* 89:873–903. http://dx.doi.org/10.1085/jgp.89.6.873

Guo, X.T., A. Uehara, A. Ravindran, S.H. Bryant, S. Hall, and E. Moczydlowski. 1987. Kinetic basis for insensitivity to tetrodotoxin and saxitoxin in sodium channels of canine heart and denervated rat skeletal muscle. *Biochemistry.* 26:7546–7556. http://dx.doi.org/10.1021/bi00398a003

Hanck, D.A., E. Nikitina, M.M. McNulty, H.A. Fozzard, G.M. Lipkind, and M.F. Sheets. 2009. Using lidocaine and benzocaine to link sodium channel molecular conformations to state-dependent antiarrhythmic drug affinity. *Circ. Res.* 105:492–499. http://dx.doi.org/10.1161/CIRCRESAHA.109.198572

Heggeness, S.T., and J.G. Starkus. 1986. Saxitoxin and tetrodotoxin. Electrostatic effects on sodium channel gating current in crayfish axons. *Biophys. J.* 49:629–643. http://dx.doi.org/10.1016/S0006-3495(86)83690-6

Heinemann, S.H., H. Terlau, and K. Imoto. 1992a. Molecular basis for pharmacological differences between brain and cardiac sodium channels. *Pflugers Arch.* 422:90–92. http://dx.doi.org/10.1007/BF00381519

Heinemann, S.H., H. Terlau, W. Stühmer, K. Imoto, and S. Numa. 1992b. Calcium channel characteristics conferred on the sodium channel by single mutations. *Nature.* 356:441–443. http://dx.doi.org/10.1038/356441a0

Henderson, R.J.M.R., J.M. Ritchie, and G.R. Strichartz. 1973. The binding of labelled saxitoxin to the sodium channels in nerve membranes. *J. Physiol.* 235:783–804.

Henderson, R., J.M. Ritchie, and G.R. Strichartz. 1974. Evidence that tetrodotoxin and saxitoxin act at a metal cation binding site in the sodium channels of nerve membrane. *Proc. Natl. Acad. Sci. USA.* 71:3936–3940. http://dx.doi.org/10.1073/pnas.71.10.3936

Hilber, K., W. Sandtner, T. Zarrabi, E. Zebedin, O. Kudlacek, H.A. Fozzard, and H. Todt. 2005. Selectivity filter residues contribute unequally to pore stabilization in voltage-gated sodium channels. *Biochemistry.* 44:13874–13882. http://dx.doi.org/10.1021/bi0511944

Hille, B. 1975. An essential ionized acid group in sodium channels. *Fed. Proc.* 34:1318–1321.

Hille, B. 1977. Local anesthetics: hydrophilic and hydrophobic pathways for the drug-receptor reaction. *J. Gen. Physiol.* 69:497–515. http://dx.doi.org/10.1085/jgp.69.4.497

Hille, B., A.M. Woodhull, and B.I. Shapiro. 1975. Negative surface charge near sodium channels of nerve: divalent ions, monovalent ions, and pH. *Philos. Trans. R. Soc. Lond. B Biol. Sci.* 270:301–318. http://dx.doi.org/10.1098/rstb.1975.0011

Horn, R., and C.A. Vandenberg. 1984. Statistical properties of single sodium channels. *J. Gen. Physiol.* 84:505–534. http://dx.doi.org/10.1085/jgp.84.4.505

Huang, C.-J., and E. Moczydlowski. 2001. Cytoplasmic polyamines as permeant blockers and modulators of the voltage-gated sodium channel. *Biophys. J.* 80:1262–1279. http://dx.doi.org/10.1016/S0006-3495(01)76102-4

Huang, C.-J., I. Favre, and E. Moczydlowski. 2000. Permeation of large tetra-alkylammonium cations through mutant and wild-type voltage-gated sodium channels as revealed by relief of block at high voltage. *J. Gen. Physiol.* 115:435–454. http://dx.doi.org/10.1085/jgp.115.4.435

Huang, L.Y., A. Yatani, and A.M. Brown. 1987. The properties of batrachotoxin-modified cardiac Na channels, including state-dependent block by tetrodotoxin. *J. Gen. Physiol.* 90:341–360. http://dx.doi.org/10.1085/jgp.90.3.341

Huang, X., F. Dong, and H.-X. Zhou. 2005. Electrostatic recognition and induced fit in the κ-PVIIA toxin binding to Shaker potassium channel. *J. Am. Chem. Soc.* 127:6836–6849. http://dx.doi.org/10.1021/ja042641q

Hui, K., G. Lipkind, H.A. Fozzard, and R.J. French. 2002. Electrostatic and steric contributions to block of the skeletal muscle sodium channel by μ-conotoxin. *J. Gen. Physiol.* 119:45–54. http://dx.doi.org/10.1085/jgp.119.1.45

Koshland, D.E. 1958. Application of a theory of enzyme specificity to protein synthesis. *Proc. Natl. Acad. Sci. USA.* 44:98–104. http://dx.doi.org/10.1073/pnas.44.2.98

Lange, A., K. Giller, S. Hornig, M.-F. Martin-Eauclaire, O. Pongs, S. Becker, and M. Baldus. 2006. Toxin-induced conformational changes in a potassium channel revealed by solid-state NMR. *Nature.* 440:959–962. http://dx.doi.org/10.1038/nature04649

Lee, C.H., and P.C. Ruben. 2008. Interaction between voltage-gated sodium channels and the neurotoxin, tetrodotoxin. *Channels (Austin).* 2:407–412. http://dx.doi.org/10.4161/chan.2.6.7429

Li, R.A., K. Hui, R.J. French, K. Sato, C.A. Henrikson, G.F. Tomaselli, and E. Marbán. 2003. Dependence of μ-conotoxin block of sodium channels on ionic strength but not on the permeating [Na^+]: implications for the distinctive mechanistic interactions between Na^+ and K^+ channel pore-blocking toxins and their molecular targets. *J. Biol. Chem.* 278:30912–30919. http://dx.doi.org/10.1074/jbc.M301039200

Liu, Y., M.E. Jurman, and G. Yellen. 1996. Dynamic rearrangement of the outer mouth of a K^+ channel during gating. *Neuron.* 16:859–867. http://dx.doi.org/10.1016/S0896-6273(00)80106-3

Llewellyn, L.E. 2006. Saxitoxin, a toxic marine natural product that targets a multitude of receptors. *Nat. Prod. Rep.* 23:200–222. http://dx.doi.org/10.1039/b501296c

Lönnendonker, U. 1989. Use-dependent block of sodium channels in frog myelinated nerve by tetrodotoxin and saxitoxin at negative holding potentials. *Biochim. Biophys. Acta.* 985:153–160. http://dx.doi.org/10.1016/0005-2736(89)90360-X

Lönnendonker, U. 1991. Use-dependent block with tetrodotoxin and saxitoxin at frog Ranvier nodes. II. Extrinsic influence of cations. *Eur. Biophys. J.* 20:143–149. http://dx.doi.org/10.1007/BF01561136

López-Barneo, J., T. Hoshi, S.H. Heinemann, and R.W. Aldrich. 1993. Effects of external cations and mutations in the pore region on C-type inactivation of Shaker potassium channels. *Receptors Channels.* 1:61–71.

Makielski, J.C., J. Satin, and Z. Fan. 1993. Post-repolarization block of cardiac sodium channels by saxitoxin. *Biophys. J.* 65:790–798. http://dx.doi.org/10.1016/S0006-3495(93)81102-0

Moczydlowski, E., S.S. Garber, and C. Miller. 1984. Batrachotoxin-activated Na^+ channels in planar lipid bilayers. Competition of tetrodotoxin block by Na^+. *J. Gen. Physiol.* 84:665–686. http://dx.doi.org/10.1085/jgp.84.5.665

Moczydlowski, E., B.M. Olivera, W.R. Gray, and G.R. Strichartz. 1986. Discrimination of muscle and neuronal Na-channel subtypes by binding competition between [^{3}H]saxitoxin and μ-conotoxins. *Proc. Natl. Acad. Sci. USA.* 83:5321–5325. http://dx.doi.org/10.1073/pnas.83.14.5321

Moran, O., A. Picollo, and F. Conti. 2003. Tonic and phasic guanidinium toxin-block of skeletal muscle Na channels expressed in mammalian cells. *Biophys. J.* 84:2999–3006. http://dx.doi.org/10.1016/S0006-3495(03)70026-5

Patton, D.E., and A.L. Goldin. 1991. A voltage-dependent gating transition induces use-dependent block by tetrodotoxin of rat IIA sodium channels expressed in *Xenopus* oocytes. *Neuron.* 7:637–647. http://dx.doi.org/10.1016/0896-6273(91)90376-B

Payandeh, J., T. Scheuer, N. Zheng, and W.A. Catterall. 2011. The crystal structure of a voltage-gated sodium channel. *Nature.* 475:353–358. http://dx.doi.org/10.1038/nature10238

Penzotti, J.L., H.A. Fozzard, G.M. Lipkind, and S.C. Dudley Jr. 1998. Differences in saxitoxin and tetrodotoxin binding revealed by mutagenesis of the Na^+ channel outer vestibule. *Biophys. J.* 75:2647–2657. http://dx.doi.org/10.1016/S0006-3495(98)77710-0

Penzotti, J.L., G.M. Lipkind, H.A. Fozzard, and S.C. Dudley Jr. 2001. Specific neosaxitoxin interactions with the Na^+ channel outer vestibule determined by mutant cycle analysis. *Biophys. J.* 80:698–706. http://dx.doi.org/10.1016/S0006-3495(01)76049-3

Ravindran, A., and E. Moczydlowski. 1989. Influence of negative surface charge on toxin binding to canine heart Na channels in planar bilayers. *Biophys. J.* 55:359–365. http://dx.doi.org/10.1016/S0006-3495(89)82813-9

Ravindran, A., L. Schild, and E. Moczydlowski. 1991. Divalent cation selectivity for external block of voltage-dependent Na^+ channels prolonged by batrachotoxin. Zn^{2+} induces discrete substates in cardiac Na^+ channels. *J. Gen. Physiol.* 97:89–115. http://dx.doi.org/10.1085/jgp.97.1.89

Reed, J.K., and M.A. Raftery. 1976. Properties of the tetrodotoxin binding component in plasma membranes isolated from *Electrophorus electricus*. *Biochemistry.* 15:944–953. http://dx.doi.org/10.1021/bi00650a002

Salgado, V.L., J.Z. Yeh, and T. Narahashi. 1986. Use- and voltage-dependent block of the sodium channel by saxitoxin. *Ann. N. Y. Acad. Sci.* 479:84–95. http://dx.doi.org/10.1111/j.1749-6632.1986.tb15563.x

Santarelli, V.P., A.L. Eastwood, D.A. Dougherty, R. Horn, and C.A. Ahern. 2007a. A cation-π interaction discriminates among sodium channels that are either sensitive or resistant to tetrodotoxin block. *J. Biol. Chem.* 282:8044–8051. http://dx.doi.org/10.1074/jbc.M611334200

Santarelli, V.P., A.L. Eastwood, D.A. Dougherty, C.A. Ahern, and R. Horn. 2007b. Calcium block of single sodium channels: role of a pore-lining aromatic residue. *Biophys. J.* 93:2341–2349. http://dx.doi.org/10.1529/biophysj.107.106856

Satin, J., J.W. Kyle, M. Chen, P. Bell, L.L. Cribbs, H.A. Fozzard, and R.B. Rogart. 1992. A mutant of TTX-resistant cardiac sodium channels with TTX-sensitive properties. *Science.* 256:1202–1205. http://dx.doi.org/10.1126/science.256.5060.1202

Satin, J., J.W. Kyle, Z. Fan, R. Rogart, H.A. Fozzard, and J.C. Makielski. 1994a. Post-repolarization block of cloned sodium channels by saxitoxin: the contribution of pore-region amino acids. *Biophys. J.* 66:1353–1363. http://dx.doi.org/10.1016/S0006-3495(94)80926-9

Satin, J., J.T. Limberis, J.W. Kyle, R.B. Rogart, and H.A. Fozzard. 1994b. The saxitoxin/tetrodotoxin binding site on cloned rat brain IIa Na channels is in the transmembrane electric field. *Biophys. J.* 67:1007–1014. http://dx.doi.org/10.1016/S0006-3495(94)80566-1

Schild, L., and E. Moczydlowski. 1991. Competitive binding interaction between Zn^{2+} and saxitoxin in cardiac Na^+ channels. Evidence for a sulfhydryl group in the Zn^{2+}/saxitoxin binding site. *Biophys. J.* 59:523–537. http://dx.doi.org/10.1016/S0006-3495(91)82269-X

Schlief, T.R., R. Schönherr, K. Imoto, and S.H. Heinemann. 1996. Pore properties of rat brain II sodium channels mutated in the selectivity filter domain. *Eur. Biophys. J.* 25:75–91. http://dx.doi.org/10.1007/s002490050020

Sheets, M.F., and D.A. Hanck. 1992. Mechanisms of extracellular divalent and trivalent cation block of the sodium current in canine cardiac Purkinje cells. *J. Physiol.* 454:299–320.

Strichartz, G., T.R. Rando, S. Hall, J. Gitschier, L. Hall, B. Magnani, and C.H. Bay. 1986. On the mechanism by which saxitoxin binds to and blocks sodium channels. *Ann. N. Y. Acad. Sci.* 479:96–112. http://dx.doi.org/10.1111/j.1749-6632.1986.tb15564.x

Sun, Y.-M., I. Favre, L. Schild, and E. Moczydlowski. 1997. On the structural basis for size-selective permeation of organic cations through the voltage-gated sodium channel. Effect of alanine mutations at the DEKA locus on selectivity, inhibition by Ca^{2+} and H^+, and molecular sieving. *J. Gen. Physiol.* 110:693–715. http://dx.doi.org/10.1085/jgp.110.6.693

Terlau, H., S.H. Heinemann, W. Stühmer, M. Pusch, F. Conti, K. Imoto, and S. Numa. 1991. Mapping the site of block by tetrodotoxin and saxitoxin of sodium channel II. *FEBS Lett.* 293:93–96. http://dx.doi.org/10.1016/0014-5793(91)81159-6

Todt, H.S.C., S.C. Dudley Jr., J.W. Kyle, R.J. French, and H.A. Fozzard. 1999. Ultra-slow inactivation in μ1 Na^+ channels is produced by a structural rearrangement of the outer vestibule. *Biophys. J.* 76:1335–1345. http://dx.doi.org/10.1016/S0006-3495(99)77296-6

Townsend, C., and R. Horn. 1997. Effect of alkali metal cations on slow inactivation of cardiac Na^+ channels. *J. Gen. Physiol.* 110:23–33. http://dx.doi.org/10.1085/jgp.110.1.23

Ulbricht, W. 2005. Sodium channel inactivation: molecular determinants and modulation. *Physiol. Rev.* 85:1271–1301. http://dx.doi.org/10.1152/physrev.00024.2004

Weigele, J.B., and R.L. Barchi. 1978. Saxitoxin binding to the mammalian sodium channel. Competition by monovalent and divalent cations. *FEBS Lett.* 95:49–53. http://dx.doi.org/10.1016/0014-5793(78)80049-0

Woodhull, A.M. 1973. Ionic blockage of sodium channels in nerve. *J. Gen. Physiol.* 61:687–708. http://dx.doi.org/10.1085/jgp.61.6.687

Worley, J.F. III, R.J. French, and B.K. Krueger. 1986. Trimethyloxonium modification of single batrachotoxin-activated sodium channels in planar bilayers. Changes in unit conductance and in block by saxitoxin and calcium. *J. Gen. Physiol.* 87:327–349. http://dx.doi.org/10.1085/jgp.87.2.327

Xiong, W., Y.Z. Farukhi, Y. Tian, D. Disilvestre, R.A. Li, and G.F. Tomaselli. 2006. A conserved ring of charge in mammalian Na^+ channels: a molecular regulator of the outer pore conformation during slow inactivation. *J. Physiol.* 576:739–754. http://dx.doi.org/10.1113/jphysiol.2006.115105

Yamamoto, D., J.Z. Yeh, and T. Narahashi. 1984. Voltage-dependent calcium block of normal and tetramethrin-modified single sodium channels. *Biophys. J.* 45:337–344. http://dx.doi.org/10.1016/S0006-3495(84)84159-4

Young, K.A., and J.H. Caldwell. 2005. Modulation of skeletal and cardiac voltage-gated sodium channels by calmodulin. *J. Physiol.* 565:349–370. http://dx.doi.org/10.1113/jphysiol.2004.081422

Zarrabi, T., R. Cervenka, W. Sandtner, P. Lukacs, X. Koenig, K. Hilber, M. Mille, G.M. Lipkind, H.A. Fozzard, and H. Todt. 2010. A molecular switch between the outer and the inner vestibules of the voltage-gated Na^+ channel. *J. Biol. Chem.* 285:39458–39470. http://dx.doi.org/10.1074/jbc.M110.132886

Zhang, M.-M., J.R. McArthur, L. Azam, G. Bulaj, B.M. Olivera, R.J. French, and D. Yoshikami. 2009. Synergistic and antagonistic interactions between tetrodotoxin and μ-conotoxin in blocking voltage-gated sodium channels. *Channels (Austin).* 3:32–38. http://dx.doi.org/10.4161/chan.3.1.7500

Zhang, M.-M., P. Gruszczynski, A. Walewska, G. Bulaj, B.M. Olivera, and D. Yoshikami. 2010. Cooccupancy of the outer vestibule of voltage-gated sodium channels by micro-conotoxin KIIIA and saxitoxin or tetrodotoxin. *J. Neurophysiol.* 104:88–97. http://dx.doi.org/10.1152/jn.00145.2010